

FINISHING OF CERAMIC BALLS BY MAGNETIC
FLOAT POLISHING WITH ONLINE
VIBRATION MONITORING
AND CONTROL

By

SRIHARI RAGHAVA RAO

Bachelor of Engineering

University of Madras

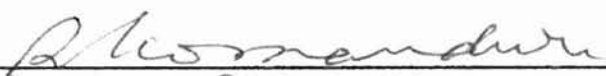
Madras, India

1997

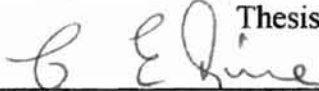
Submitted to the Faculty of the
Graduate College of the
Oklahoma State University
in partial fulfillment of
the requirements for
the Degree of
MASTER OF SCIENCE
December, 1999


FINISHING OF CERAMIC BALLS BY MAGNETIC
FLOAT POLISHING WITH ONLINE
VIBRATION MONITORING
AND CONTROL

Thesis Approved:



Thesis Adviser







Dean of the Graduate College

SUMMARY

A Polishing shaft was designed to polish a batch of $17/32''$ ceramic (Si_3N_4) balls by magnetic float polishing with the use of non-diamond abrasives such as B_4C , SiC and CeO_2 . For polishing purposes, the polishing chamber needs to be aligned with the polishing chamber. The manual method employed in aligning the chamber with the polishing shaft gives way to problems of non-repeatability and inconsistency. Because of this it is possible that a particular run may not produce the desired effect of reducing the sphericity of the balls. A method to detect a faulty set-up by monitoring the vibrations generated during polishing has been given. The vibration from the polishing apparatus is recorded with the help of two accelerometer pick-ups, and are sent to Vibroport 41, a vibration-monitoring device, to convert the recorded vibrations to Frequency spectrum Vs time graphs. It has been observed that the lobes or waviness on the surface of the balls, due to high out-of-roundness values, act as vibration generators during polish. Accordingly it has been observed that high out-of-roundness values of the balls being polished generate vibrations with higher amplitude when compared to balls with lower out-of-roundness values. Hence the amplitude of vibrations Vs sphericity of balls curve drawn shows that the amplitude of vibration decreases linearly with decrease in sphericity of balls. Any discrepancy

in the linearly decreasing trend indicates a faulty set-up and the polishing run can be stopped without deteriorating the sphericity of the ceramic balls any further. This technique can be very useful to prevent wastage of magnetic fluid, abrasives, ceramic ball material and time by indicating an improper set-up with the help of vibrations generated during polishing.

ACKNOWLEDGEMENTS

I would first like to thank my adviser, Dr. Ranga Komanduri, for his guidance and advice throughout this work. I would like to thank Dr. C. E. Price, and Dr. H. B. Lu for serving in my graduate advisory committee. I wish to express my sincere gratitude to Dr. Young Bae Chang for his valuable assistance to this work. I would like to show my appreciation to Dr. Jiang Ming and Mr. Peijun Cao, former research assistants at MAERL, OSU, for their support. Special thanks to Mr. Ashok Lakshmanan for assisting me in performing the polishing. I would like to thank Mr. Mukund Ravikumar, Mr. Vijaykumar Raman, Mr. Ashutosh Khuperkar and Mr. Beeram Sreekanth Reddy, for their co-operation, help and valuable discussions.

I am indebted to my family Mrs. L. Sona Bai, Mr. L. R. Rao, Mrs. R. Premasudha, Mr. R. Sriram, Ms. R. Srividya and Mrs. R. Saraswathi who were always encouraging me in times of need, and without whose support, it would not have been possible for me to have come this far. Finally I would like to acknowledge one and all who have helped me towards the completion of this work.

This project is sponsored by grants from the National Science Foundation (NSF) on "Tribological Interactions in Polishing of Advanced Ceramics and

Glasses," (CMS - 9414610), and "Design, Construction and Optimization of Magnetic Field Assisted Polishing," (DMI - 9402895) and DoD's DEPSCoR program on "Finishing of Advanced Ceramics," (DAAH04 - 96 - 1 - 0323) and CATT's program on "Finishing Silicon Nitride Balls for Bearing Applications," (Contract No. F34601 - 95 - D - 0376).

TABLE OF CONTENTS

1	Introduction	1
	Traditional finishing method for ceramic balls	2
2	Literature Review	5
	Literature on Magnetic Float Polishing	5
	Literature on vibration measurement in rolling element bearings	11
3	Problem Statement	17
4	Approach	20
	Introduction	20
	Salient features of Magnetic Float Polishing technology	21
	Work material for ceramic balls – Silicon Nitride	24
	Abrasives	27
	Evaluating roundness by number	30
	Vibration monitoring equipment – Vibroport 41	34
	Accelerometer pick-up (AS-020)	36
	Experimental work	37
5	Design of Polishing Shaft	39
	Constraints in designing the polishing shaft	39
	Final design and considerations	40

6	Methodology of finishing silicon nitride balls	44
	Apparatus for Magnetic Float Polishing	45
	Polishing conditions and procedure	47
	Mechanical polishing	51
	Chemo-mechanical polishing	52
	Precision manufacturing process	54
7	Vibration monitoring and control	59
	Introduction	59
	Validating set-up using vibration	60
	Set-up for online vibration monitoring	62
	Parameters	64
8	Results and Discussion	67
	Analysis made with respect to amplitude	85
	Manual method of calculating the amplitudes	86
	Analysis of Amplitude Vs Sphericity curve	87
9	Conclusions	92
10	Future work	95
	Setting up of the polishing apparatus using lasers	95
	Vibration monitoring and control using advances software	96
	References	98

LIST OF TABLES

A	Chemical composition and typical properties of NBD-200 Silicon Nitride ball	28
B	Abrasives considered for use in Magnetic Float Polishing	29
C	Properties of abrasives used and Test conditions for polishing process	50

LIST OF FIGURES

1.1	Schematic of conventional V-groove lapping method for finishing steel or ceramic balls.	3
2.1.1(a)	Plots of the response of each polishing parameter level on Ra.	8
2.1.1(b)	Plots of the response of each polishing parameter level on Rt.	8
2.1.2(a)	Plots of the S/N ratios of showing the effect of each parameter level on the surface finish Ra.	9
2.1.2(b)	Plots of the S/N ratios of showing the effect of each parameter level on the surface finish Rt.	9
2.2	Schematic of Vibration tester.	14
4.1	The four different reference circles available for evaluating roundness.	31
4.2	Schematic diagram of electronic measuring system.	33
5.1	Final design of the polishing shaft.	43
6.1	Schematic of Magnetic Float Polishing technique.	46
7.1	Set-up for online vibration monitoring and control.	63
8.1	Typical background vibration of the environment in which polishing was performed.	68
8.2	Frequency spectrum recorded during the first 15-minute interval during the 14 th polishing run.	69
8.3	Frequency spectrum taken for the last 15-minute interval of the 14 th polishing run.	70

8.4	Frequency spectrum taken during the first 15-minute interval of the 27 th polishing run.	72
8.5	Frequency spectrum taken during the last 15-minute interval of the 27 th polishing run.	73
8.6	Frequency spectrum taken during the first 15-minute interval of the 31 st polishing run.	74
8.7	Frequency spectrum taken during the second 15-minute interval of the 31 st polishing run.	75
8.8	Frequency spectrum taken during the last 15-minute interval of the 31 st polishing run.	76
8.9	Sphericity of the balls after the 14 th polishing run.	78
8.10	Sphericity of the balls after the 27 th polishing run.	78
8.11	Sphericity of the balls after the 31 st polishing run.	79
8.12	Frequency spectrum of the first 15 minutes of the polish test run done with an under-sized spindle.	80
8.13	Frequency spectrum of the second 15-minute interval of the polish test run done with an under-sized spindle.	81
8.14	Graph of Sphericity of balls Vs Amplitude of vibration.	88
8.15	Comparison of Frequency spectrum Vs time graph with Sphericity	91

Chapter 1

Introduction

Steel ball bearings are used for bearing applications mainly in many mechanical and aerospace industries. The main disadvantage of steel ball bearings is that they need to be adequately lubricated for satisfactory operation and optimum life. In spite of the mentioned disadvantages, the steel ball bearings were used for numerous applications, until the arrival of high-speed spindles for machining centers. Speeds up to 180,000 rpm are easily attainable with these high-speed spindles. Traditional steel ball bearings have been found to fail much before their specified life, with use in such high-speed spindles. Advanced ceramics are now being considered for use in bearing applications. Advanced ceramic balls are used in hybrid bearings, which are made up of ceramic balls and steel races. Such hybrid bearings can operate at very high speeds and high temperatures with very minimal or no lubrication. The life of hybrid bearings is 2 to 3 times the life of an all-steel bearing in high-speed applications. Silicon nitride (Si_3N_4) is an advanced ceramic material that satisfies the requirements for a ceramic ball material. It has high toughness, high stiffness (elastic modulus), and high hardness.

1.1 Traditional finishing method for ceramic balls

Ceramic balls are finished in the industry by V-groove lapping, which is the same technique used for finishing steel balls. This process uses high load (~10N/ball), low speed, and expensive diamond abrasives for finishing ceramic balls. The schematic of this process is given in fig 1.1. Due to the use of low speeds (~50 rpm), the process takes about 12 to 16 weeks to finish the ceramic balls from its as-received condition to finish. Moreover the hard and expensive diamond abrasives used create a number of surface imperfections on the balls. This is due to the fact, that diamond abrasives (harder than any ceramic) is used at very high loads and low speeds. This causes the formation of pits, gouges and other surface imperfections. Since advanced ceramic materials are very hard and brittle, the presence of such surface imperfections during operation gives rise to nucleation sites for cracks. Since the rate of fatigue crack propagation is very high in ceramics, the balls fail catastrophically during operation.

In order to prevent such failures, the surface imperfections have to be minimized as much as possible, even if it is impossible to completely remove them. Therefore a new technique to polish ceramic balls which uses low loads, higher speeds, and abrasives slightly harder or even less harder than the ceramic material used has been developed to improve the surface quality of the finished balls. Magnetic Float Polishing (MFP) is a technique for finishing ceramic balls by the application of low loads (~1 N/ball), high speeds (~ 2000 – 5000 rpm), and abrasives such as boron carbide (B_4C), silicon carbide (SiC), and cerium oxide

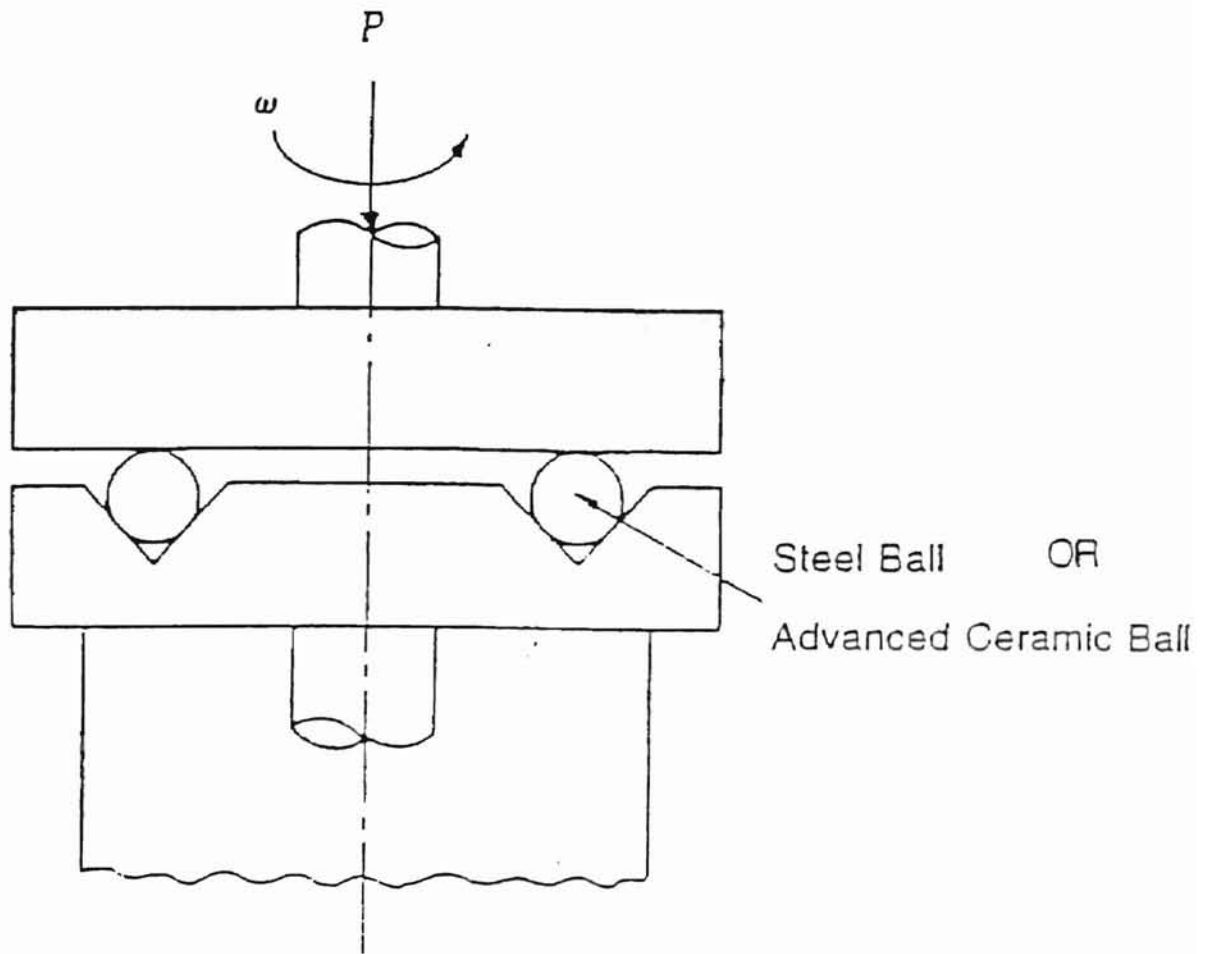


Figure 1.1: Schematic of V-groove lapping for finishing steel or ceramic balls

(CeO₂). The procedure for magnetic float polishing has been given in chapter 6. Chapter 2 deals with a review of the literature published in the field of MFP and in the field of vibration measurement in rolling element bearings. The problem statement is dealt with in chapter 3. Chapter 4 deals with the approach taken in conducting this work. This chapter also explains the principle and working of some important instrumentation and devices used in this work. The constraints and methodology adopted for designing the polishing shaft has been given in chapter 5. The need, construction and set-up used for monitoring vibrations has been given in chapter 7. The results of the vibration measurements have been discussed in chapter 8. Chapter 9 and 10 deal with the conclusions arrived and some suggestions for future work.

Chapter 2

Literature Review

2.1 Literature on Magnetic Float Polishing

Umehara and Kato [1990] made a major breakthrough in polishing of ceramic balls by introducing the concept of a float, and hence the name Magnetic Float Polishing (MFP). Earlier [Tani and Kawata, 1984] polishing of ceramic balls using magnetic force was done without any float. This resulted in very low force and low material removal. The usage of a float resulted in increase in polishing force, leading to higher removal rates. The freely rotating float also enables a three point contact to the ball (float, chamber wall, and polishing shaft), so that the ball moves around a fixed center, leading to improvements in sphericity. MFP is still in the research stages under the active involvement of Dr. R. Komanduri in the USA. The following is a review of the literature in the field of magnetic float polishing.

Komanduri et al [1996] studied the possibility of chemo-mechanical action in magnetic float polishing of silicon nitride, using chromium oxide and aluminum oxide abrasive. Since aluminum oxide and chromium oxide abrasives are nearly of the same hardness, magnetic float polishing tests were conducted on silicon nitride balls with these two abrasives to investigate mechanical versus chemo-mechanical aspects of polishing. It was observed that even though Al_2O_3

and Cr_2O_3 have almost the same hardness, the material removal rates on Si_3N_4 balls was found to be different. The higher removal rate with chromium oxide over aluminum oxide is attributed due to chemo-mechanical action of chromium oxide with silicon nitride. Observation of the balls finished with aluminum oxide showed pits, possibly formed by abrasion, brittle fracture and dislodgment of grains, but after polishing with chromium oxide, a relatively smooth surface was observed (with fewer pits) possibly due to chemo-mechanical action.

Ming Jiang and Komanduri [1997] investigated the finishing of Si_3N_4 balls by magnetic float polishing (MFP) process. The authors identified three necessary stages for polishing, namely, initial roughing stage where the emphasis is on high material removal rate with minimal surface-subsurface damage, intermediate semi-finishing stage where material removal rate, sphericity, and surface roughness have to be closely monitored, and final finishing stage with emphasis on the required size, sphericity and finish. High material removal rates ($1 \mu\text{m}/\text{min}$) with minimal subsurface damage are possible using harder abrasives, such as B_4C or SiC due to rapid accumulation of minute amounts of material removed by mechanical micro-fracture at high polishing speeds and low loads in the MFP process.

Ming Jiang and R Komanduri [1998] investigated the chemo-mechanical polishing (CMP) of Silicon Nitride balls with various abrasives, to find out their effectiveness in producing a good surface finish. Among the abrasives investigated for CMP of Si_3N_4 balls, CeO_2 and ZrO_2 were found to be most

effective followed by Fe_2O_3 and Cr_2O_3 . Thermodynamic analysis (Gibbs free energy of formation) indicated the formation of SiO_2 layer on the surface of Si_3N_4 balls with these abrasives. This is particularly true in water environment which facilitates chemo-mechanical interaction between abrasive and work material by participating directly in the chemical reaction leading to the formation of a softer SiO_2 layer. It was found that there exists very little, if any, of CMP occurring in an oil-based polishing environment. The conductivity and dissolution value of an oil-based polishing fluid is nearly zero and the oil film between the abrasive and the work-material prevents any chemical reaction between them as well as the removal of the reaction layer formed, if any, thus minimizing CMP.

Ming Jiang and Komanduri [1998] conducted tests to obtain optimum polishing conditions using Taguchi Method. An orthogonal array was used in the tests, and the three parameters for surface quality were identified as polishing force, abrasive concentration, and polishing speed. The tests indicated that polishing force was the most significant factor for overall surface finish. The results from the Taguchi experimental design also indicated that within the range of parameters evaluated, a high level of polishing force (1.4N/ball), a low level of abrasive concentration (5%), and a high level of polishing speed are optimum for improving both Ra and Rt. A surface finish of 15 nm Ra and 150 nm Rt was obtainable with SiC abrasive (1 μm), and it was observed that further improvement in surface finish is possible by chemo-mechanical polishing, using

CeO₂ abrasive. Figures 2.1.1 and 2.1.2 show the conclusions of the work in form of graphs.

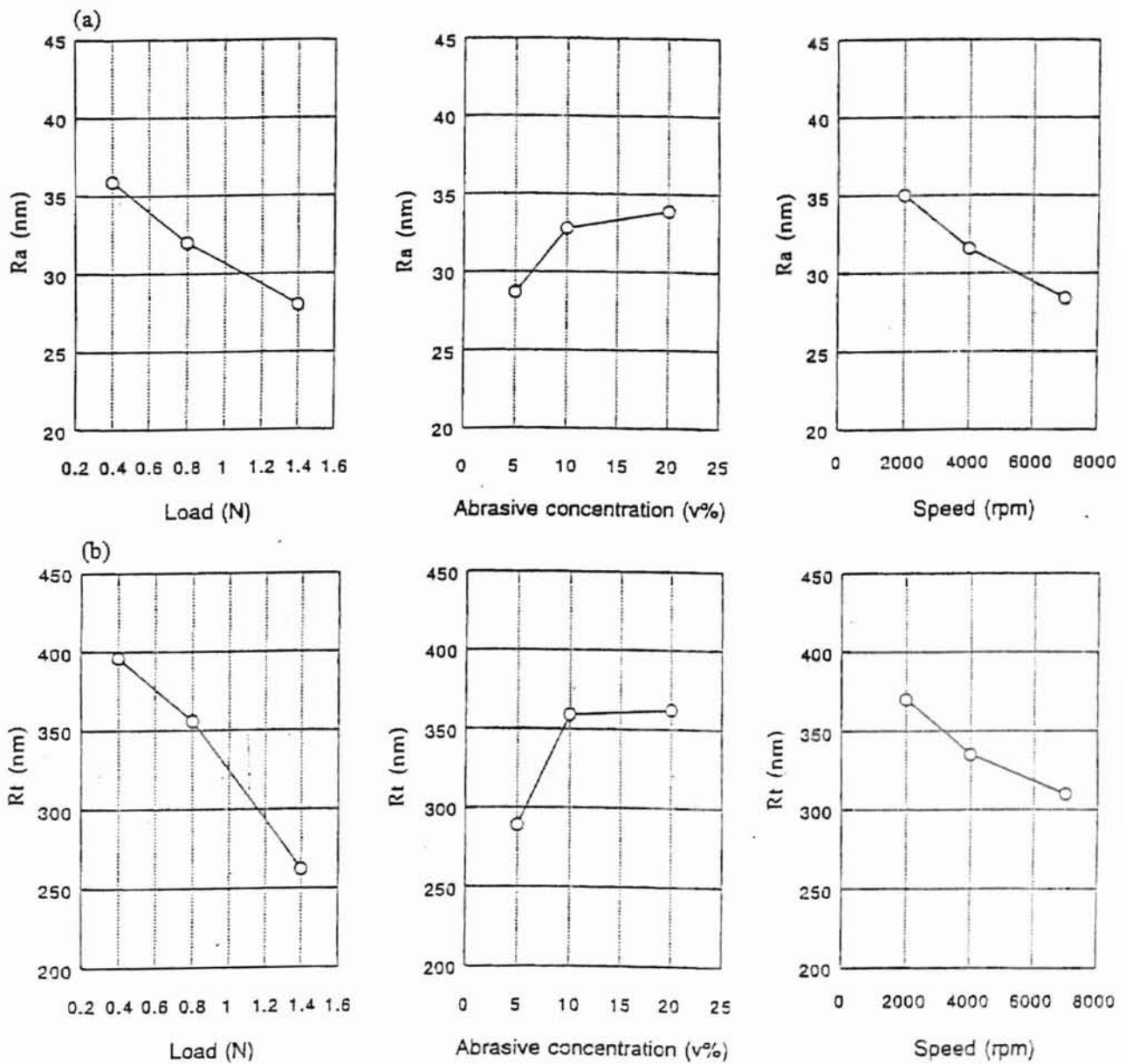


Figure 2.1.1(a) Plots of the response of each polishing parameter level on Ra.
 (b) Plots of the response of each polishing parameter level on Rt. [Jiang and Komanduri, 1998]

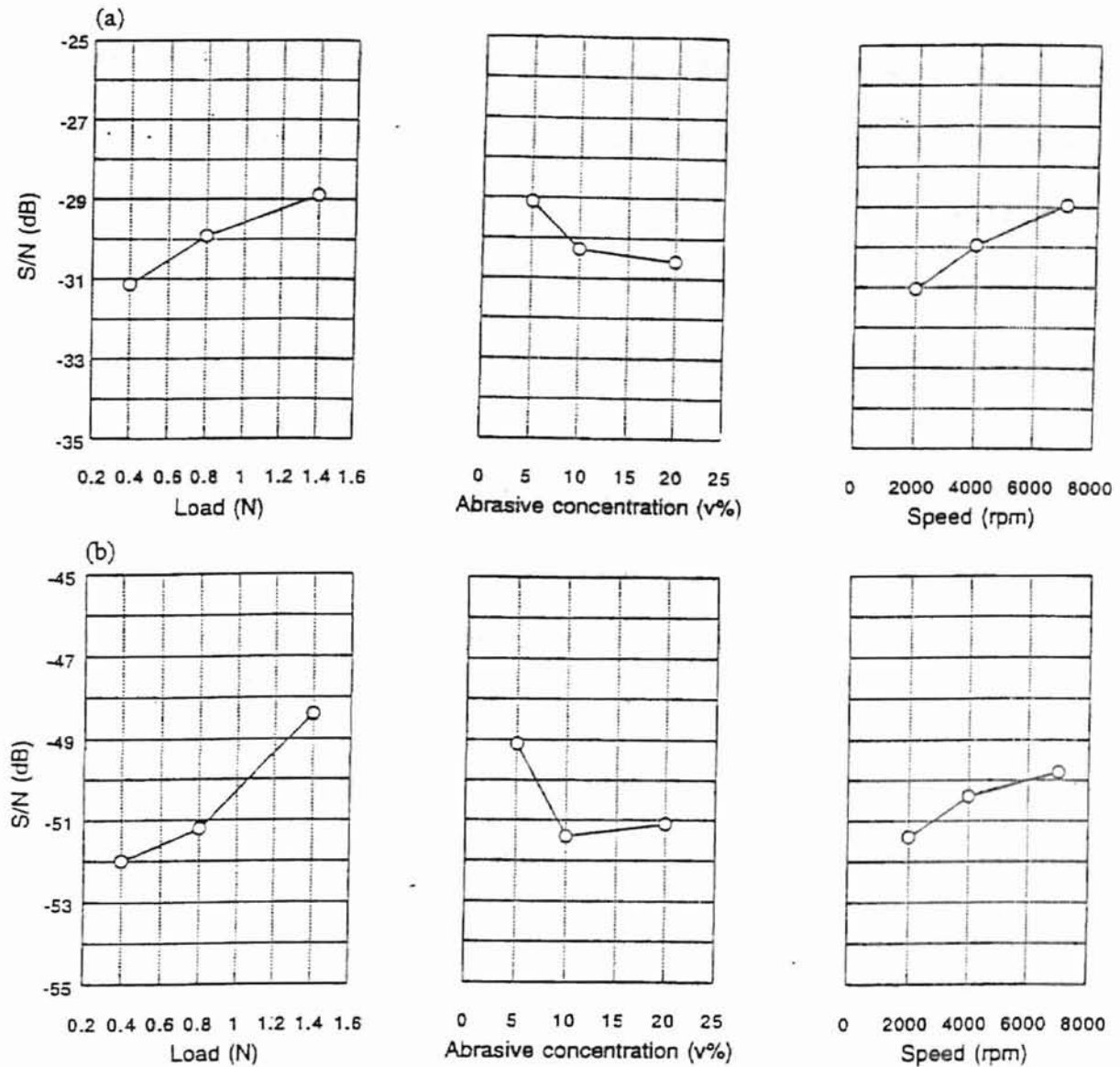


Figure 2.1.2 (a) Plots of the S/N ratios showing the effect of each parameter level on the surface finish Ra.

(b) Plots of the S/N ratios showing the effect of each parameter level on the surface finish Rt. [Jiang and Komanduri, 1998]

The success of a polishing run can be defined as its ability to reduce the sphericity of the ball by removing material equally throughout the surface of the ball. This depends on a number of factors, which have to be monitored before each and every polish. They include alignment of the polishing chamber and polishing shaft, condition of the groove formed on the shaft, condition of the rubber on the chamber wall, the groove formed on the float and the sphericity of the balls before the polish. Of these, the most important factor for reducing the sphericity of the balls is the first one mentioned viz. alignment of the polishing chamber with the polishing shaft. This setting is currently done manually, giving rise to problems of non-repeatability and inconsistencies. Since the contacting surface of the balls and the shaft is tapered, any misalignment of the two axes will cause the balls to contact the tapered surface in a line not perpendicular to the axis. Hence the load on the balls will not be uniform all around the shaft but will be varying between a high and a low value. Due to varied load, the spinning motion of the ball is not uniform around the chamber during polishing resulting in non-uniform material removal around the surface of the ball. This gives rise to high sphericity values.

The next important factor is the condition of the groove on the shaft. If the groove is bigger than the surface of contact of the balls, there is a possibility that the balls may be able to move laterally or radially within the width of the groove. At high speeds of polishing, the ball may hit the shaft and the walls of the chamber frequently. This is unacceptable since it may affect the sphericity of the

balls. In this case, the shaft must be machined before any further polishing, to ensure improvement in sphericity of the balls. The groove on the rubber and the float should be monitored to make sure that the rotation of the balls takes place without any difficulty due to the size and width of the groove. If such a condition is observed, it is a good practice, to change the required component.

2.2 Literature on Vibration measurement in rolling element bearings

Any manufacturing or polishing process can be characterized by monitoring the vibrations given out during the process. Vibration can be analyzed in different forms with the available form of output. Vibration studies have been done on machines and structures, mainly aircraft, to ensure that no cracks are present in the wing spans or whether a bearing is in good condition or not. Studies were done on machining to deduce the surface finish of the machined part, as the machining takes place. Based on a history of vibration readings of a bearing, taken over a time period, one can determine the condition of the bearing, whether it is suitable for use or not. The usual method of characterizing a vibration is by a frequency spectrum. A frequency spectrum is a plot of component amplitudes as a function of frequency. It may be possible to relate the peak frequencies to rotating unbalance (in case of rotating machinery) to one or more of the rotating elements. A frequency plot is more useful than either a mean value or a RMS value, since these plots often indicate discrete

frequencies that are related to specific machine components and operating characteristics. The frequency spectrum also contains significant amplitude information that may be useful to the engineer in judging significant system behavior in order to rate operating condition, to make a redesign, to plan corrective action and such. Various studies have been done by authors on the problem of bearing vibration and noise due to surface imperfections like waviness, on both the rolling element as well as the bearing races.

Vance [1988] discusses the application of vibration in detecting specific problems associated with roller bearings and other rotors. In his book he insists that vibration analysis is a very effective tool for detection and analysis of bearing problems. The rolling element bearing generates discrete frequencies that can be calculated using specific design and operating information like pitch diameter, ball diameter, number of elements, contact angle and shaft speed. These calculated frequencies align with peaks in the vibration spectrum when defects in the bearing are present.

Tallian and Gustafsson [1965] conducted extensive research on rolling bearing vibration research and control. They determine the effect of rolling bearing vibrations on machine noise, experimentally. They also developed an analytical model for the bearing, as a vibration generator and used it to identify forcing frequencies, resonant frequencies, and amplitude relationships. They classify the outer ring vibrations in ball bearings, primarily into two classes of vibration sources, identified as cyclic variations in the compliance of the bearing

to the load (present even in geometrically perfect bearing) and vibrations generated due to rolling over geometrical imperfections. All other vibration sources are considered to be secondary in contributing to outer ring vibrations. They indicate that it is possible to control the geometry of bearing components purposefully, and to predict the vibration of the assembly when the parts geometry is known. Amplitudes of vibration, in addition of frequencies, can be computed. It has been found that the relative magnitude of vibrations, in different measuring directions, is different. The magnitude of axial vibration in the low frequencies (of about 500-cps) are generally considerably higher than in the radial direction, whereas they are approximately the same at high frequencies. However it has been found that this is strongly influenced by the mounting of the bearing.

Yhland [1967-68] indicates that the surface properties of the raceways of rings and rolling bodies are of great influence on the state of vibration in an assembly. He claims that it is not generally possible to predict frequencies and amplitudes of vibrations caused by geometrical imperfections in a rolling bearing. He discusses a method of solving the problem, by developing a simple and objective vibration testing method and, as a complement, a method for detecting geometrical imperfections. A vibration set up as shown in the figure 2.2 is used. When the inner ring rotates, the waviness, or the geometrical imperfection, of the bearing elements generates vibrations in the outer ring. The radial part of the vibratory motion at a point on the outer perimeter of the latter

ring is measured by a velocity sensitive pick-up. He mentions that it is not possible to accurately estimate the vibrations caused by the bearings of an

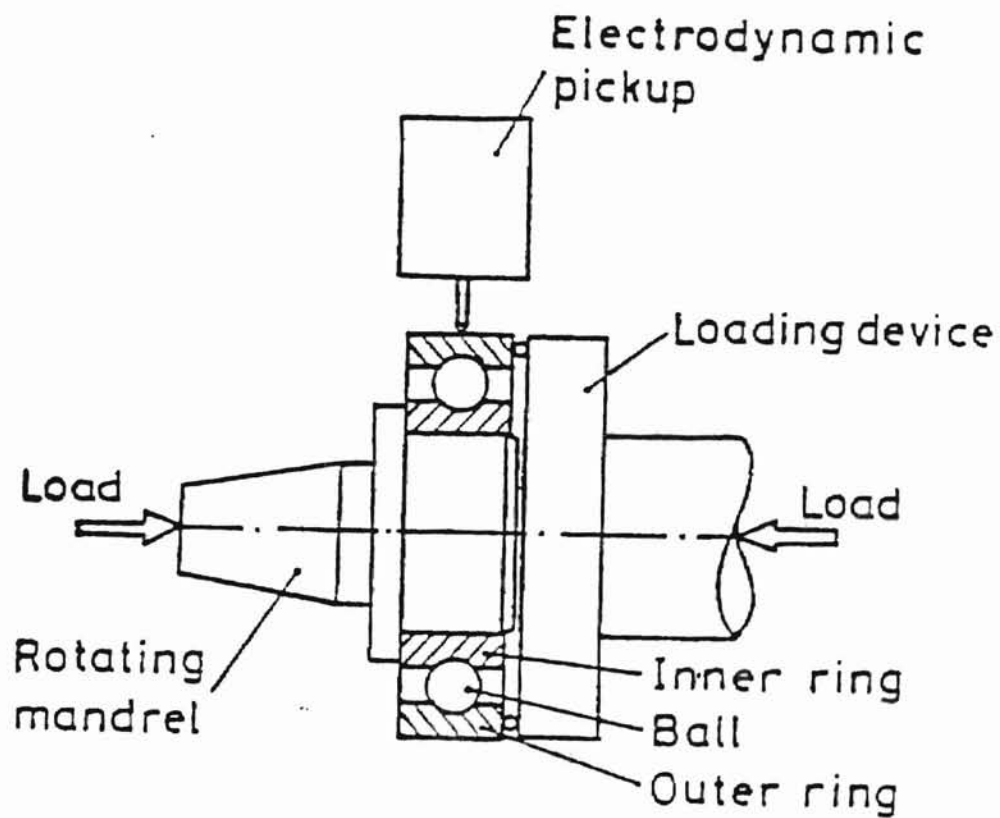


Figure 2.2: Schematic view of the vibration tester. [Yhland, 1967-68]

assembly, if the vibration characteristics of the bearings are known from measurements in the test. But the testing method is an objective one and is capable of separating the bad bearings from the good. It has been mentioned that due to the presence of many other vibration sources in common assemblies, the difference between bad and good bearings is more pronounced in this type of test.

Tallian [1958] suggested that bearing vibrations were attributed primarily to relative displacements of the bearing rings as a consequence of geometrical imperfections of rolling surface termed "waviness". This encompasses the periodic components of radial deviations, from perfect surfaces of rotation, in the harmonic orders of approximately 1 to 100 waves per circumference. The surface roughness constitutes imperfections of much higher order and was considered to be of little influence. It was postulated, from the mathematical model available, that the relation between waviness and vibration amplitudes would in general be linear, and that higher orders of waviness caused higher frequency vibrations.

The basis of the work presented here has thus been based on the lines of literature given above. Instead of determining whether a bearing is good or not depending on the vibration of the outer race, the validity of the set up in reducing the sphericity of the balls for a particular polish is determined with the vibration recorded during polishing. The polishing set up can be considered as a ball bearing, with the polishing shaft as the inner race, and the chamber walls to be the outer race. Since the loads applied are very low (~ 1 N/ball) the out-of-

roundness of the balls act as vibration generators during polishing. Hence an aim of this work is to show that the amplitude of vibration decreases with decrease in out-of-roundness of the balls. Since this is a gentle and flexible polishing technique, the amplitude of vibration will be comparatively lesser than those of ball bearings. The rubber sheet on the wall of the polishing chamber and, to a lesser extent, the polishing fluid, acts as vibration dampers. The magnitude of vibration damping is not discussed in this work. Since the condition is same for all the tests, the damping effect is not considered. !

Problem Statement

Magnetic float polishing is performed in Si_3N_4 balls with magnetic fluid and ceramic abrasives. This process is performed to obtain the best possible surface finish and sphericity of the balls. As mentioned earlier it is an aim of this work to design a spindle to finish 17/32" balls to a sphericity of at least $0.4 \mu\text{m}$. Various constraints like dimensions of the existing chamber, the size of the balls, and the thickness of the rubber guide ring in the chamber have been taken as the main constraints in designing the polishing shaft.

The setting of the polishing chamber concentric with the polishing shaft is a very important requirement for the polishing to be valid. Validity of a set-up can be defined as the ability of the set-up to improve or sustain the sphericity of the balls, without any deterioration, during that particular polish. A faulty set-up (eccentricity between the polishing shaft and the polishing chamber axes) can cause deterioration in sphericity, as well as loss of material of the ball. This setting is currently done with the help of a Vernier caliper manually, and the possibility of an offset, however minute, between the chamber and the spindle is unavoidable. Hence a method to analyze the validity of set-up using vibrations recorded with the help of two accelerometers has been the main thrust of this work. Vibroport 41, a vibration-monitoring device, and two accelerometers AS-

020, provided by Schenck, have been used in conducting these experiments. The polishing runs were of 1-hour duration, within which 3 frequency spectrums for both the accelerometers were obtained. The results will be analyzed relative to the previous runs based on sphericity of the balls obtained. The frequency spectrums of selected runs will be discussed with the sphericity of the balls and the conditions used, in comparison with other runs. An effort will be taken to correlate the amplitude of vibration obtained with the sphericity of the balls and the method undertaken to calculate the values in the graphs will be discussed.

Hence the primary objectives of this work is to

1. Design a polishing shaft to finish 17/32" (final diameter) Si_3N_4 balls for a chamber capable of finishing a batch of 13 balls to the required out-of-roundness and surface quality, by Magnetic Float Polishing technique.
2. Perform polishing on the balls from the as-received size to about 150-200 μm from the finish size, with emphasis on material removal, using non-diamond abrasives such as B_4C and SiC .
3. Control the out-of-roundness (also called as sphericity) and material removal rate of the balls by gradually reducing the size of the abrasives used from coarse to fine.
4. Improve the surface quality of the balls by employing chemo-mechanical polishing, after polishing with B_4C and SiC , using CeO_2 abrasive, which is softer than Si_3N_4 material, in water based magnetic fluid environment.

5. Monitor the vibrations of the run during the process using Vibroport 41, vibration monitoring equipment, with acceleration pickups, to ascertain the effectiveness of the run in improving the sphericity and surface quality, when compared to previous runs using a frequency spectrum (Frequency Vs Time Vs Amplitude).
6. Analyze and discuss the results of the frequency spectrum with respect to the sphericity of the polished balls. This in turn provides information on an objective basis, about the alignment of the chamber and the polishing spindle about their axes.
7. Provide some guidelines to be observed during the run on whether the run will improve the sphericity of the balls or not, and stop it before more material gets removed in an improper set up.
8. Analyze the results based on amplitude of vibration and draw graph between amplitude of vibration and sphericity, and to deduce whether a linear relationship exists between them.

Chapter 4

Approach

4.1 Introduction

This investigation lays major emphasis on finishing of 17/32" balls in a chamber designed to hold a batch of 13 balls and to conduct vibration analysis of the polishing process. A spindle will be designed to polish these balls in a chamber, taking into consideration, the various constraints involved including dimension, weight and compatibility to the existing chamber. Initial polishing, will be done by magnetic float polishing, with emphasis on material removal. Chemo-mechanical polishing will be performed on the balls to improve their surface quality. The set up during polishing plays an important role in determining the finish and quality of the balls. Vibration will be monitored for both these main stages, during polishing, to determine the validity of the run in improving the sphericity of the balls. The vibration during polishing will be characterized in the form of a 3-dimensional frequency spectrum (Frequency Vs Amplitude Vs Time), which will be analyzed during the run to ascertain whether it will yield good results even before the run is complete. A comparison will be made between frequency spectrum of different runs and the resulting sphericity from those runs.

Magnetic float polishing technique was used to polish the silicon nitride balls. The advantages of magnetic float polishing when compared to conventional V-groove method has been given in the following paragraphs.

4.2 Salient features of magnetic float polishing technology

The magnetic float polishing technology that has been developed has the following characteristics.

1. High material removal rate
2. Excellent surface finish
3. Good sphericity

In addition, the apparatus designed can handle small batches which are particularly useful when only a few balls need to be polished either due to customers demand or due to small amount of material available for evaluation during the materials development program. The process does not use diamond abrasive and is faster by an order of magnitude or more than conventional V-groove lapping process. Some of these features will be elaborated in the following.

4.2.1 High material removal rate

The material removal by polishing or lapping is due to sliding at the contact region between the workpiece and the abrasives embedded in the tool.

The material removal rate during the magnetic float polishing of ceramic balls is high because there is more sliding in this process than in conventional lapping due to following two reasons (1) The polishing load in magnetic float polishing is ~100 times lower than in conventional lapping. Hence the frictional force at the contact region is significantly reduced. Consequently, there is more sliding than rolling and (2) The drive speed in magnetic float polishing is 100 times higher than in conventional lapping. Thus there will be more sliding taking place in the polishing region due to increased relative speed. The experimental results show that the material removal rate in polishing of ceramic balls by magnetic float polishing method is ~ 50 – 100 times higher than by conventional V-groove lapping method.

4.2.2 Excellent surface finish

It is reasonable to expect that the ceramic balls finished by magnetic float polishing technology would be without the surface as well as sub-surface damage because magnetic buoyant force during polishing is extremely small (~1N/ball) and controllable. Also, the chemo-mechanical polishing with a softer abrasive is applied to this process during the final stage to improve the surface finish. The hardness of the abrasive used in chemo-mechanical polishing is about the same or much lower than that of the work material. The material removal from the ceramic balls is due to the removal of the reaction product during

chemo-mechanical polishing by frictional action. The chemical reaction is produced by the interaction between the selected abrasive, the work material, and the water from water-based ferro-fluid. Thus the resulting surface on the polished ceramic ball is extremely smooth and damage free.

4.2.3 Good sphericity

The mechanism for the generation of good sphericity on the balls, be it by lapping or magnetic float polishing, is that when the larger diameter portion of a ball enters the contact area, the load on it will increase and a larger amount of material will be removed from this place. This process continues till the expected spherical surface is obtained when the abrading tracks are uniformly distributed over the whole ball surface.

In conventional ball lapping, the material from the balls is removed by the V-groove lapping, and the recycle of the balls (i.e., from the output of the container to the input of the groove plate and from the output of the groove plate to the input of the container) is not only for automatic feeds but also for changing the lapping contact position. The ball is re-input into the groove randomly, therefore the lapping track over the whole ball surface is random and thus is uniform, so that the sphericity can be improved after lapping. In magnetic float polishing, there are 3 contact points to each ceramic ball to bring two main motions: rotation around the axis parallel to the contact area and the spinning

around the axis vertical to the contact area. The rotation of the ball is the motion for polishing and the spinning motion is the feed for polishing. The polishing track all around the ball is uniform due to its spinning motion during polishing. Thus a good sphericity can be obtained by magnetic float polishing.

4.3 Work material for Ceramic balls – Silicon Nitride

Silicon nitride (Si_3N_4) material is a ceramic with predominantly covalent bonding and hexagonal structure [McColm, 1983; Katz et al, 1985]. The electronic configuration of Si [$3s^23p^2$] (excited electron state: sp^3 hybridization) yields the usual tetrahedral arrangement of covalent bond formation with four N atoms producing a SiN_4 tetrahedral building unit, and these tetrahedral units from the hexagonal Si_3N_4 by each corner (nitrogen atoms $2s^22p^3$) being shared with two other SiN_4 tetrahedrons. So, in the three-dimensional silicon nitride network, each silicon atom is covalently bonded with four nitrogen atoms, and each nitrogen atom is covalently bonded with three silicon atoms.

Silicon nitride has two crystalline phases ($\alpha - \text{Si}_3\text{N}_4$ and $\beta - \text{Si}_3\text{N}_4$ respectively) in the microstructure. They are both covalently bonded hexagonal structured materials but $\beta - \text{Si}_3\text{N}_4$ grain is more elongated than that of $\alpha - \text{Si}_3\text{N}_4$ ($\alpha - \text{Si}_3\text{N}_4$: $a=0.78$ nm, $c=0.56$ nm; $\beta - \text{Si}_3\text{N}_4$: $a=0.76$ nm, $c=0.29$ nm). The $\alpha - \text{Si}_3\text{N}_4$ is easier to form than $\beta - \text{Si}_3\text{N}_4$ but it gets converted to $\beta - \text{Si}_3\text{N}_4$ at high temperature (1400 - 1800°C). In general, advanced silicon nitride engineering materials are $\beta -$

Si_3N_4 because all α - Si_3N_4 transform to β - Si_3N_4 during the shaping process (hot pressing).

The covalent solid has a low concentration of vacancies and cannot be sintered to high densities merely by heating. Several techniques, such as chemical vapor deposition (CVD), reaction bonding, hot pressing (HP), and hot iso-static pressing (HIP) have been available to obtain dense silicon nitride material [McColm, 1983]. These techniques will be briefly reviewed in the following.

4.3.1 Chemical Vapor Deposition (CVD) process

In the chemical vapor deposition process, pyrolytically deposited Si_3N_4 is formed from SiCl_4 vapor and NH_3 gas. The volatile SiCl_4 and NH_3 gases react and deposit the Si_3N_4 on the hot substrate. High density Si_3N_4 can be obtained, but they are usually thin and amorphous (at 0°C : $\text{SiCl}_4 + 6 \text{NH}_3 \rightarrow \text{Si}(\text{NH})_2 + 4\text{NH}_4\text{Cl}$; at 1200°C : $n\text{Si}(\text{NH})_2 \rightarrow a\text{-Si}_3\text{N}_4$).

4.3.2 Reaction bonding process

Reaction bonding of Si_3N_4 material is obtained by heating silicon in a nitrogen atmosphere. Silicon powder is compacted to high density in an inert atmosphere and then heated in a nitrogen atmosphere at $\sim 1400^\circ\text{C}$ to achieve Si_3N_4 material. The advantage of this method is that complex shapes can be

made. But the final product has about 20% porosity and 300 MPa flexural strength (at 1400°C: $3\text{Si} + 2\text{N}_2 \rightarrow \alpha\text{-Si}_3\text{N}_4$).

4.3.3 Hot Pressed and Hot Iso-statically Pressed (HIP) Process

Hot pressed Si_3N_4 material is made from a mixture of α and β Si_3N_4 powders sintered to a high density using either uniaxial or iso-static high pressure. The Si_3N_4 powders are mixed with densification aids, such as MgO or Y_2O_3 , to enable liquid phase sintering and then heated to 1700°C at 20 MPa pressure for HP and heated above 1700°C in a nitrogen atmosphere at higher pressures greater than 300 MPa for HIP. The high-pressure nitrogen gas can yield the iso-static compression, which results in a uniform material. The disadvantage of this method is high cost and only a few shapes of the product can be made. For making bulk products such as balls for bearing application, this technique is commonly used. The chemical composition and typical properties of NBD-200 silicon nitride ball ($\beta\text{-Si}_3\text{N}_4$, uniaxially pressed with 1 wt.% MgO as main sintering aid) used in this study are shown in Table A [Jiang, 1998]. A glassy phase is created at the grain boundaries during the high-temperature sintering or hot pressing of Si_3N_4 due to the reaction of Si_3N_4 and SiO_2 with small amounts of MgO . This complex glassy phase for sintering is primarily a magnesium silicate modified by Ca, Fe, Al and other impurities initially present in Si_3N_4 .

4.4 Abrasives

Abrasives considered for use in polishing are listed in the Table B [Jiang, 1998]. They are classified into two groups, one predominantly for mechanical polishing and the other for chemo-mechanical polishing depending on their mechanical hardness (higher or less than work material) and chemical activity with respect to the work material in a given environment. Fine grain size diamond, boron carbide (B_4C) and silicon carbide (SiC) abrasives which are harder than Si_3N_4 work material are used for mechanical polishing with high material removal rates to reach the desired diameter and geometry rapidly. The material removal in this case is considered to be by mechanical micro-fracture. Aluminum oxide (Al_2O_3), chromium oxide (Cr_2O_3), zirconium oxide (ZrO_2), silicon oxide (SiO_2), cerium oxide (CeO_2), iron oxide (Fe_2O_3), yttrium oxide (Y_2O_3), molybdenum oxide (Mo_2O_3) whose hardness is close to or less than Si_3N_4 work material come under the second group. Cerium oxide was found to be the most suitable ceramic for chemo-mechanical polishing of Si_3N_4 work material to improve the final surface finish.

Table A

Chemical composition and typical properties of NBD-200 silicon nitride ball

[Jiang, 1998]

Chemical composition of NBD-200 Si₃N₄ ball [Hah, et al, 1995]

Mg	Al	Ca	Fe	C	O	Si ₃ N ₄
0.6 - 1.0	≤0.5	≤0.04	≤0.17	≤0.88	2.3 - 3.3	94.1 - 97.1

Mechanical and thermal properties of Si₃N₄ ball [Hah, et al, 1995]

PROPERTY	VALUE
Flexural Strength, MPa	800
Weibull Modulus	9.7
Tensile Strength, MPa	400
Compressive Strength, GPa	3.0
Hertz Compressive Strength, GPa	28
Hardness, Hv (10kg), GPa	16.6
Fracture Toughness, K _{1c} , MNm ^{-3/2}	4.1
Density, g/cm ³	3.16
Elastic Modulus, GPa	320
Poisson's Ratio	0.26
Thermal Expansion Coefficient at 20-1000°C, /°C	2.9 x 10 ⁻⁶
Thermal Conductivity at 100°C, W/m-K	29
Thermal Conductivity at 500°C, W/m-K	21.3
Thermal Conductivity at 1000°C, W/m-K	15.5

Table B

Abrasives considered for use in Magnetic Float Polishing [Jiang, 1998]

ABRASIVE	HARDNESS	
	Mohs	Knoop kg/mm ²
Diamond	10	7000
Boron Carbide (B ₄ C)	9.3	3200
Silicon Carbide (SiC)	9.2	2500
Aluminium Oxide (Al ₂ O ₃)	9	2150
Chromium Oxide (Cr ₂ O ₃)	8.5	1800
Silicon Nitride (Si ₃ N ₄)	8.5	1600
Zirconium Oxide (ZrO ₂)	8	1200
Silicon Oxide (SiO ₂)	7	820
Cerium Oxide (CeO ₂)	6	-
Iron Oxide (Fe ₂ O ₃)	6	-
Yttrium Oxide (Y ₂ O ₃)	5.5	700
Copper Oxide (CuO)	3.5	225
Molybdenum Oxide (Mo ₂ O ₃)	1.5	-

4.5 Evaluating roundness by number

The numerical value of the out of roundness is the maximum peak-to-valley height (P+V). There are four different reference circles available for this calculation: Least square circle (LS), minimum zone circle (MZ), maximum inscribed circle (MI), and minimum circumscribed circle (MC) as shown in figure 4.1. The roundness of the balls was measured using TalyRond 250 in this study. The least square circle is the arithmetic average of the deviations from the mean or reference circle. Minimum zone circle consists of two concentric circles with least possible gap in between them enclosing all the points within the two circles. Maximum inscribed circle is the largest possible circle that can be enclosed by all the points of the reading. Minimum circumscribed circle is the smallest possible circle that encloses all the points of the measured ball.

4.5.1 TalyRond 250

TalyRond 250 is a computer controlled stylus instrument manufactured by Rank Taylor Hobson Inc (UK). It has a stylus, a variable inductance pick-up (transducer) with rotating worktable (for roundness measurement) and a vertical straightness unit (for vertical straightness measurement). It has two motorized axes for measurement (the worktable and the vertical straightness unit) and one motorized axis for stylus contact. It can evaluate roundness, vertical straightness, squareness, parallelism, flatness, co-axiality, cylindricity, concentricity, eccentricity and runout and is capable of conducting harmonic analysis. The

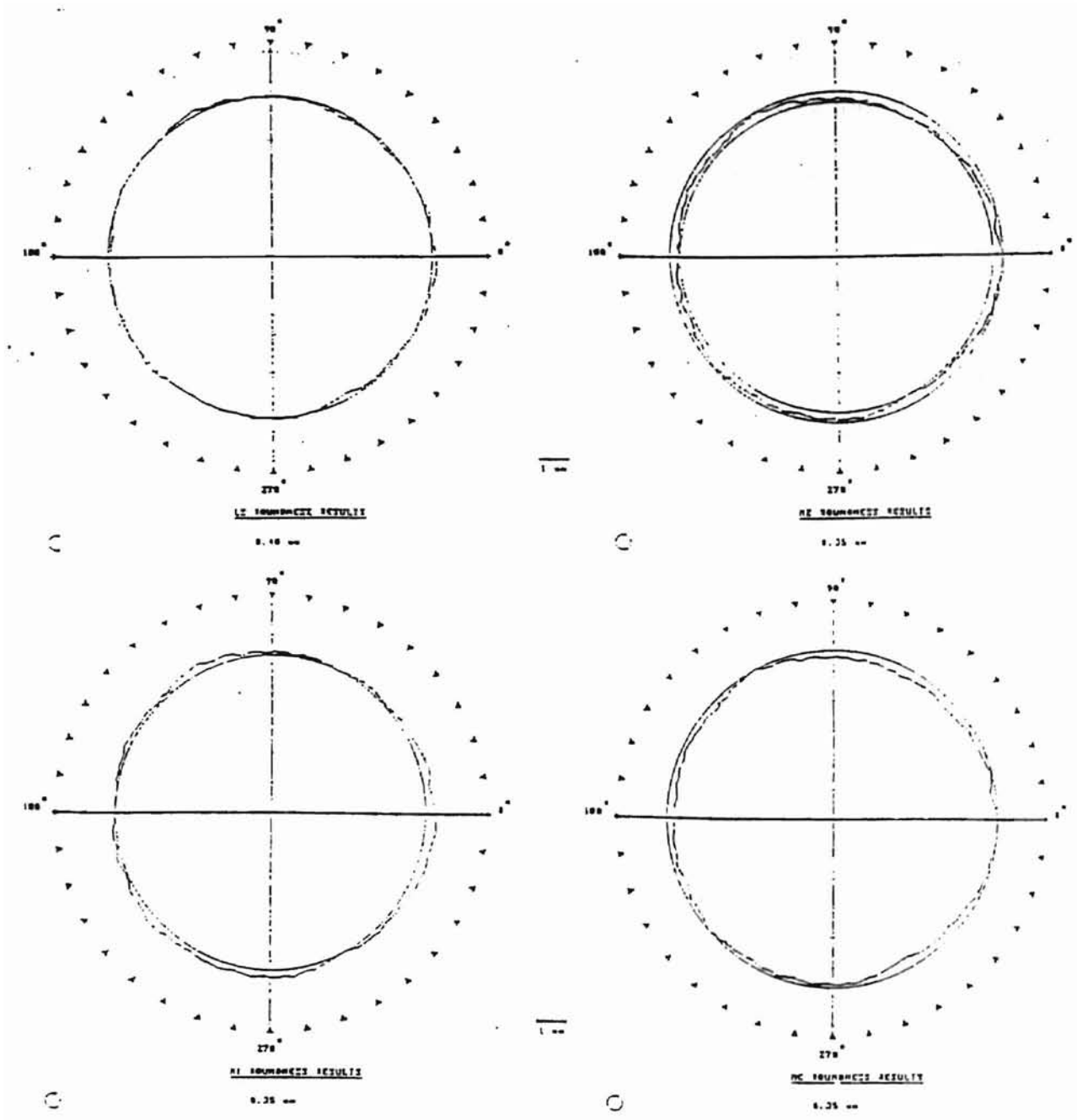
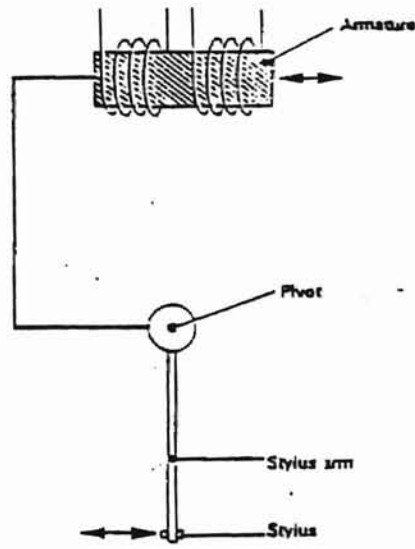


Figure 4.1: Different types of reference circles used in measurement of sphericity of balls

roundness limit of error from the worktable and pick-up spindle is about $0.05 \mu\text{m}$ ($0.04 \mu\text{m} + 0.0003 \mu\text{m}/\text{mm}$ height over the worktable).

The deviation from spherical form is determined by rotation of the ball against the transducer with several grams gauge force. The stylus tip, a sapphire ball with a diameter of 2.0 mm, contacts the surface being measured which is fixed on the rotating worktable. When the worktable rotates, the roundness deviation will cause minute movements of the stylus. The variable inductance pickup will convert this movement of the stylus into variations of an electrical signal. As shown in figure 4.2, the variable inductance pick-up is the armature that is connected to the stylus and can move between the two coils when the stylus moves. This will alter their inductance. These two coils are connected to an AC bridge circuit, the movement of the armature will unbalance this bridge and will then give an output proportional to the movement. The signal is amplified and fed to a recorder. The phase signal, which depends on the direction of movement, is compared with the oscillator to determine in which direction the recorder pen will move from its zero (balance) position. 2CR (2 – stage CR networks) type filter with a cut-off of 50 upr (undulations per revolution) is used in this study. The 2CR filter has 75% of their true value. The amplitudes of irregularities with longer wavelength are progressively reduced but that of the amplitudes of irregularities with shorter wavelength will almost remain unchanged. This filter, which suppresses the out-of-roundness lobes (undulations with approximately equal height and spacing) and leaves the



Principle of variable inductance pick-up

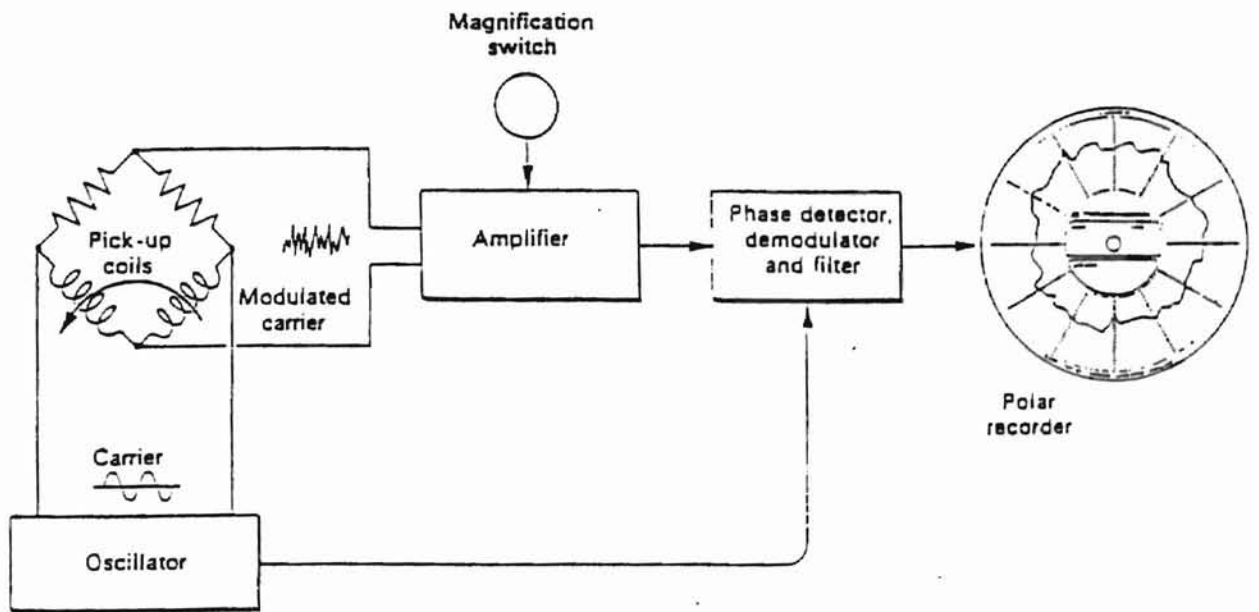


Figure 4.2: Schematic diagram of electronic measuring system

general shape unchanged. It will allow the other surface irregularities to be displayed at higher magnification.

4.6 Vibration monitoring equipment – Vibroport 41

Vibroport 41 is a portable, dual-channel instrument that is designed to perform various tasks such as shaft vibration, bearing vibration, frequency spectrum, tracking analysis, and balancing for machine diagnostics and predictive machine maintenance. Only frequency spectrum has been used for this experiment, and hence other functions of the equipment will not be discussed here. The frequency spectrum can be displayed as an averaged spectrum, where the type and number of averages can be specified. The display can also be done with respect to time and speed. The user can specify the speeds or the time intervals at which the frequency spectrum is required. In this experiment a spectrum is retrieved every 3 minutes (180 seconds) for a total of 5 spectrums. An accelerometer pick-up (AS-020), whose construction and working will be discussed later, was used for measurement of vibration. It is possible to make use of two accelerometer pick-ups simultaneously to measure vibrations at two different locations on the machine. The two pick-ups are connected to two separate channels on the equipment, for evaluating the frequency spectrum. The result obtained can be compared with a reference, which is usually located away from the machine. The equipment allows the user to perform set-up of the

parameters either automatically or manually. In this case the set-up was performed manually and the parameters set were

Input:	Active
Type of Pick-up:	Acceleration
Sensitivity:	100 mV/g
Amplitude Unit:	m ² /s; rms
Amplitude Range:	Auto
Frequency Range:	0 – 2 kHz
Number of lines:	400
Window:	Flat top

The amplitude range is set as auto to enable the instrument to capture the maximum frequency and scale the other frequencies down accordingly. The frequency range is the maximum and minimum frequencies at which the instrument is to capture and display the vibration signature. The number of lines, along with the maximum and minimum frequencies, determines the resolution on the spectrum, where

$$\text{Resolution} = (F_{\max} - F_{\min}) / \text{no. of lines}$$

A flat top filter is a DSA window function, which provides the best amplitude accuracy for measuring discrete frequency components, when compared to other window functions, was chosen. The results are printed out using an in-built printer on a thermally sensitive paper.

4.7 Accelerometer pick-up (AS-020)

The accelerometers provided by Schenck, function according to the piezoelectric principle. Inside the transducer, a stiff spring applies a pre-load to a piezo-ceramic disk and a mass. When a vibration is introduced, an alternating load is exerted by the mass upon the crystal or disk, which, in turn, creates electric charges as a result of the piezo-effect. The change of the magnitude of the charge is proportional to the acceleration. The charge is converted into a voltage signal by a charge amplifier. These accelerometers are specially designed for rough industrial applications. The casing is made of high quality stainless steel and is hermetically sealed. Damage to the transducer from the shock is prevented by integral overload protection. Thermal insulation and special temperature compensation in the charge amplifier suppress temperature influences on the signal. This assures accurate readings over a wide temperature range. Two accelerometer pick-ups with machine mountable screws were used.

4.8 Experimental work

- The polishing shaft was driven by a high-speed, high-precision air bearing spindle (PI spindle) with a step-less speed regulation of up to 10,000 rpm.
- The magnetic field was measured using a Gauss/Tesla meter.
- The polishing load was set up, by measuring the normal force, with a Kistler's piezoelectric dynamometer connected to a charge amplifier and a display (resolution 0.02N).
- The weight of abrasives to be used for polishing, which is 10% of the volume of magnetic fluid used for that polish, was found using a precision balance from Brinkman Instruments (resolution: 0.1mg).
- The ball diameter was measured using a digital micrometer from Mitutoyo (resolution: 1 μ m).
- Full characterization of the bearing balls is required. This includes the size (specific diameter), size variation, sphericity, and surface finish. In this investigation, three balls are randomly selected from each batch and each ball is traced 3 times in approximately three orthogonal planes. The roundness or sphericity was measured using TalyRond 250 and surface roughness using Form Talysurf 120L. According to ABMA, the sphericity of each ball is defined from the maximum value of the roundness measured on three orthogonal planes of the ball. Similarly, the surface finish of each ball is taken as the maximum value of three traces along three orthogonal planes of the ball.

- The roundness of the balls was measured using TalyRond 250 (cut off: 50 upr, Filter: 2CR). The out-of-roundness trace measures the maximum departure (maximum peak-to-valley height) from a true circle and as such it's denoted roundness. The surface finish of the balls was not measured, as it was not considered to be important to this work.
- Vibration readings are taken for each polish during finishing of a batch of 13 17/32" balls. A frequency spectrum Vs time graph with a total of 5 frequency Vs amplitude graphs given out at 3-minute interval is taken for every 15 minutes. A total of 3-frequency spectrum Vs time graphs is taken for every 1-hour polish, taking into account, the time taken for printing the graphs.

Design of polishing shaft

The main aim of this work was to polish $17/32''$ ceramic balls on the existing apparatus, which was never tried before. The existing polishing shaft is suitable for polishing only $9/32''$ size balls. Hence a new polishing shaft had to be designed for polishing $17/32''$ balls. Finishing of ceramic balls of size $9/32''$ was done previously with the help of a stainless steel chamber. It was not an aim of this work to design a new chamber for polishing $17/32''$ ceramic balls. So the dimensions of the existing chamber was taken as the main constraint in designing the polishing shaft.

5.1 Constraints in designing the polishing shaft

The polishing chamber, used for polishing $9/32''$ sized balls, is of the form of a hollow cylinder supported by a base. The inner diameter of the chamber is $2.9''$ and its depth is $\sim 4''$. A bank of permanent magnets (Nd-Fe-B, Residual magnetization 10500 Gauss) with alternate N and S magnets, is placed below the stainless steel chamber. The polishing shaft has to be fitted to a PI air spindle with the help of four screws. The PI air spindle has a free end for the polishing shaft to be attached. The free end has a diameter of about $1.9''$ with 4 screw holes at a PCD of $1.5''$, 90° apart. The weight of the polishing shaft has to be as

minimum as possible to reduce lateral vibrations, when rotating at very high speeds. The size of the balls to be polished is one main consideration in designing of the polishing shaft. The outer and inner diameters of the polishing shaft have to be connected by a 30° inclination to facilitate a 3-point contact between the float and the walls of the chamber and the polishing shaft. Previous researchers found out, that an inclination of 30° provides the best possible results when compared to other inclination angles. The outer and inner diameters have to be calculated, by taking into consideration, the point on the inclined surface at which the ball will contact the polishing shaft. This design should be done for the final diameter of the balls, with the point of contact, approximately at the center of the inclination. As the diameter of the balls reduces due to polishing, the point of contact moves away from the center. If the design is done taking into consideration, the as-received diameter of the ball, it is possible that during final polishing stages, the ball may not contact the polishing shaft on the inclined surface. X ?

5.2 Final design and considerations

Magnetic float polishing of ceramic balls provides good results, if the point of contact of the balls with the polishing shaft lies on the inclined surface throughout the polish, from the as-received diameter to the finishing diameter. However during polishing, the balls form a groove on the inclined surface of the polishing shaft and on the float. This groove acts as a guide way for the balls to

rotate at high speeds during polishing. Care has to be taken to ensure that the groove formed lies within the inclined surface during the entire duration of finishing the balls. Thus for dependable polishing of ceramic balls, it is advisable to have separate spindles for different ball diameters. The outer diameter (OD) of the polishing shaft was decided based on the diameter of the chamber and the diameter of the balls. It is obvious that the OD of the polishing shaft should be less than the diameter of the chamber (2.9"). For the ball to contact the inclined surface approximately at the center, and to finish balls slightly more or less ($\pm 100\mu\text{m}$) than the final diameter, the gap between the chamber and the OD of the polishing shaft has to be at-least less than half the diameter of the balls ($\text{OD} \leq 0.5 * \text{Dia of balls}$). This was calculated to be 2.31".

The inner diameter (ID) of the polishing shaft was arrived upon, by taking into consideration the thickness of the iso-propylene rubber sheet on the walls of the chamber and the diameter of the balls. Hence ID is the sum of the thickness of the rubber sheet and diameter of the walls on either side of the diameter of the chamber ($\text{ID} = [\text{Dia of balls} + \text{thickness of rubber sheet}] * 2$). Since the PCD of the bolt circle on the PI spindle is 1.5" and the ID of the polishing shaft was calculated to be 1.56", a recess was made to enable access to the holes. The diameter was fixed at 2.1", slightly more than the sum of PCD and diameter of the hole. The upper surface of the polishing shaft has to be strictly perpendicular to the axis of the PI spindle to facilitate accurate mating of the two surfaces. The outer surface of the polishing shaft has to be parallel to the axis of the spindle to

avoid excessive vibrations due to out-of-roundness of the polishing shaft. Appropriate tolerances were fixed, and an inward taper, proceeding from the OD to the ID, of 30° was fixed between the outer and inner diameters. The total height of the polishing shaft was fixed at 3". The final diagram of the polishing shaft has been given in figure 5.1.

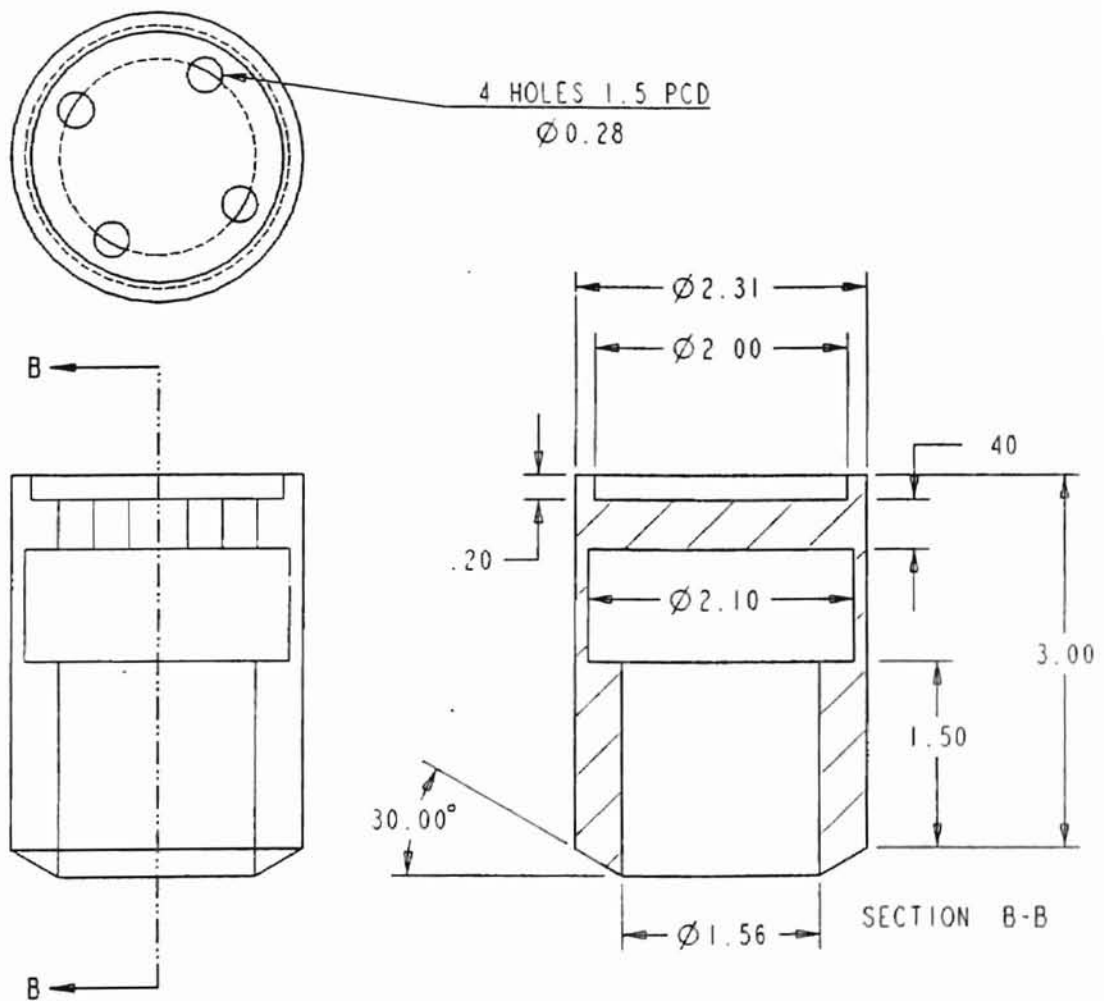


Figure 5.1: Final design of the polishing shaft.

Chapter 6

Methodology of finishing silicon nitride balls

The methodology of Magnetic Float Polishing (MFP) involving mechanical polishing followed by chemo-mechanical polishing, for the finishing of Si_3N_4 balls from the as-received condition is discussed in this chapter. It involves mechanical removal of material initially using harder abrasives (with respect to the work material) of different materials of progressively lower hardness and finer grain sizes followed by final chemo-mechanical polishing (CMP) using preferably a softer abrasive for obtaining superior finish with minimal surface or sub-surface defects, such as scratches, micro-cracks, or pits on the Si_3N_4 balls. High material removal rates ($1 \mu\text{m}/\text{min}$) with minimal sub-surface damage is obtained with harder abrasives, such as B_4C or SiC (relative to Si_3N_4) due to the use of a flexible support system, small polishing loads ($\sim 1 \text{ N}/\text{ball}$), and fine abrasives but high polishing speeds (compared to conventional polishing) by rapid accumulation of minute amounts of material removed by micro-fracture. Final polishing of Si_3N_4 balls using a softer abrasive, such as CeO_2 (that chemo-mechanically reacts with the Si_3N_4 work material) results in high quality Si_3N_4 balls of bearing quality with superior surface finish ($R_a < 15 \text{ nm}$, $R_t < 150 \text{ nm}$) and damage-free surface. CMP is very effective for obtaining excellent

surface finish on Si_3N_4 ceramic material and CeO_2 in particular is one of the most suitable materials for this application.

6.1 Apparatus for magnetic float polishing

The magnetic float polishing (MFP) technique is based on the magneto-hydrodynamic behavior of a magnetic fluid that can float non-magnetic materials, such as abrasives suspended in the magnetic fluid. The force applied by the abrasive on the part is extremely low (1N/ball) and highly controllable. Figure 4.1 shows the schematic diagram of magnetic float polishing apparatus used for finishing of advanced ceramic balls. A bank of permanent magnets (Nd-Fe-B, Residual magnetization 10500 Gauss) with alternate N and S are arranged below a stainless steel float chamber. The float chamber is filled with the required amount of magnetic fluid with 5 – 10% of abrasive. The magnetic fluid is a colloidal dispersion of extremely fine (100 to 150 Å) sub-domain ferromagnetic particles, usually magnetite (Fe_3O_4), in a carrier fluid, such as water or kerosene. It is made stable against particle agglomeration by coating the surface of the particles with an appropriate surfactant. In this investigation, a water base magnetic fluid (W-40) is used (Saturation Magnetization at 25°C; 400 Gauss, Viscosity at 27°C is 25 Cp).

When magnetic field is applied, the magnetic particles in the magnetic fluid are attracted downward to the area of higher magnetic field and an upward buoyant force is exerted on all non-magnetic materials to push them to the area

of lower magnetic field. The abrasive grains, the ceramic balls, and the acrylic float inside the chamber (all being non-magnetic materials) are floated by the magnetic buoyant force. A drive shaft is lowered to make contact with the balls and to press them down to reach the desired level of force or height. The balls are

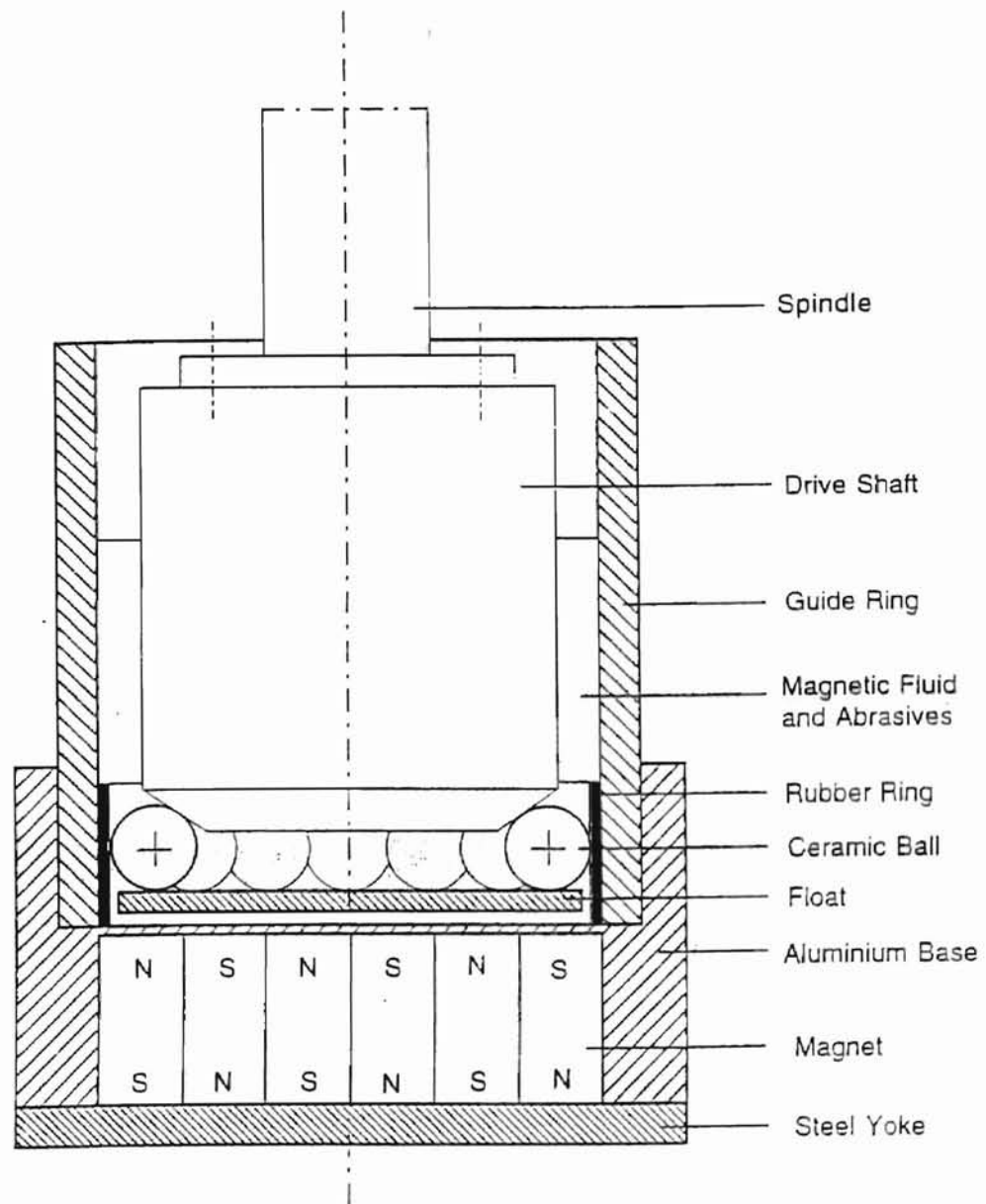


Figure 6.1: Schematic of Magnetic float polishing technique

held by three-point contact between the float chamber wall, the float and the drive shaft and polished by the abrasive grains under the action of the magnetic buoyancy as the spindle rotates. Damage-free surface on ceramic balls is obtained, by magnetic float polishing technique, because low and controlled magnetic buoyant force (1N/ball) is applied via the flexible float. The function of the acrylic float used here is to produce more uniform and larger polishing pressure (i.e. the larger buoyancy force near the magnetic poles can be transmitted to the polishing area by this float). A urethane rubber sheet is bonded on the inner guide ring to protect it from wear. The material of the drive shaft is austenitic stainless steel (non-magnetic material).

6.2 Polishing conditions and procedure

The as-received Si_3N_4 balls (CERBEC NBD-200 from Norton Advanced Ceramics) had a nominal diameter of 14.3 mm. These balls also contained nearly a 200 μm thick x 5mm wide band of material around the periphery at the parting plane resulting from the uni-axial pressing process. These balls have to be finished to a final size of about 13.5mm (17/32"), a sphericity of at least 0.4 μm and best finish achievable. All the three factors were considered in the finishing of Si_3N_4 balls in this chapter with emphasis on the former aspect, namely, the sphericity. The large differences in the diameter between the as-received condition to the final size required is to remove all the reaction material that is

formed on and near the surface during the hot pressing process. The nominal chemical composition and the mechanical properties of NBD-200 Si_3N_4 balls have been given in chapter.

The table B [Jiang, 1998] gives properties of the various abrasives used in Magnetic Float Polishing. As in most finishing operations, there are three stages involved in magnetic float polishing (MFP) of Si_3N_4 balls, namely, a) roughing to remove as much material as possible without imparting serious damage to the surface, b) an intermediate stage of semi-finishing where size, sphericity, and surface roughness have to be carefully monitored, and c) final finishing where all three, namely size, sphericity and finish have to be closely controlled to meet the requirements.

Table C lists the conditions used for different stages of polishing. Two coarser, harder abrasives B_4C (500 grit) and SiC (800 grit) (compared to Si_3N_4 work material) were used during the initial stages of polishing to reach the desired diameter at high removal rates and at the same time improve the sphericity to facilitate proper ball motion. After reaching the diameter close to the desired diameter, an intermediate (semi-finishing) stage is utilized as a transition between the roughing and finishing stages, as the material removal rate is of prime concern in the first stage and surface finish in the final stage. The two harder abrasives with finer grit size were chosen for this intermediate stage, namely, SiC (1000 grit) and SiC (1200 grit). During this stage, the removal rates are much lower and the finish much better than roughing but the emphasis

during this stage is the improvement of sphericity. In the final stage (prior to CMP), fine B₄C abrasive (1500 grit) is used to approach the required diameter and sphericity and remove almost all the deep valleys from the surface. This is followed by final polishing using a softer, chemo-mechanical abrasive, namely, CeO₂ to produce the balls of required diameter, sphericity, and final surface finish which is extremely smooth and almost damage free by preferential removal of the peaks from the surface.

The polishing shaft in MFP apparatus was driven by a high-speed, high-precision air bearing spindle (PI spindle) with a step-less speed regulation up to 10,000 rpm. The magnetic field was measured with a Gauss/Tesla meter. The pH value of the polishing environment was measured with a pH/Temperature meter. The polishing load was set up, by measuring the normal force, with a Kistler's piezoelectric dynamometer connected to a charge amplifier and a display. To calculate material removal rates, the weight reduction in the balls can be measured by weighing the balls before and after polishing at every stage test using a precision balance. The roundness of the balls was measured using TalyRond 250. The surface finish of the polished balls, which was not considered very important for this work, was not measured.

In this study, the finished balls are characterized for roundness using a TalyRond 250 (cut-off: 50 μ m, filter: 2CR). Three balls are randomly selected from each batch, and are traced 3 times at approximately three orthogonal planes using the TalyRond. It measures the maximum departure from a true circle of

Table C

Properties of abrasives used in this work

Abrasive	Density g/cm ³	Knoop Hardness kg/mm ²	Elastic Modulus GPa	Melting Point °C
B ₄ C	2.52	2800	450	2450
SiC	3.2	2500	420	2400
CeO ₂	7.13	625	165	2500

Test conditions used for polishing process

Stage	Abrasive		Abrasive Vol %	Speed rpm	Load N/ball	Time hrs	Remarks
	Type	Grit Size					
1	B ₄ C	500	10	3000	1.0	1.0	Roughing (High material removal)
	SiC	800	10	3000	1.0	1.0	
2	SiC	1000	10	3000	1.0	1.0	Semi-finishing (Sphericity & roughness)
	SiC	1200	10	3000	1.0	1.0	
3	B ₄ C	1500	10	3000	1.0	1.0	Final finishing (Size, sphericity & finish)
	CeO ₂		10	3000	1.2	1.0	

assumed magnitude and as such it's denoted roundness. The sphericity of each ball, according to ABMA, is defined as the maximum value of the roundness measured on the three orthogonal planes of the ball. Similarly, the surface finish of each ball is taken as the maximum value of three traces along three orthogonal planes of the ball.

6.3 Mechanical polishing

The mechanism of material removal from Si_3N_4 balls by finer grit, harder abrasives, such as B_4C and SiC in MFP process is by mechanical micro-fracture because of higher hardness of the abrasive and the inherent brittleness of the work material. Under these conditions material removal occurs not by grain pullout, grain fracture and large fracture, but by micro-fracture due to cleavage. While chemo-mechanical action may also occur, its contribution is considered to be much smaller than the mechanical action, namely micro-fracture by cleavage.

Childs et al [1995] have shown that in magnetic float polishing (MFP), material removal from the balls is accomplished by the action of the abrasives embedded in the shaft due to sliding at the contact area between the drive shaft and the ball. It is unlikely that when fine abrasives are held between the Si_3N_4 balls and the stainless steel shaft that the abrasives will get embedded in the shaft, as in the present case. If this were so, one would never be able to remove material from softer work materials with loose abrasives. In an actual situation, the abrasive will abrade the soft stainless steel shaft, much more so, than the

Si_3N_4 work material and it appears unlikely that the abrasives will be embedded as Childs et al [1995], considered. Instead would be moving relative to the polishing shaft forming abrasion marks in the shaft. In fact wear on the stainless steel shaft is as a result of it and may have to be ground periodically to improve sphericity.

For larger sized abrasives and higher loads, as in conventional polishing with diamond abrasive, the finished surface is effected by the formation of deep pits, grooves and cracks. This will not be the case with finer abrasives and lighter loads. Higher material removal rates without subsurface damage is feasible by magnetic float polishing because of high polishing speeds and very flexible float system used. The low loads used (1 N/ball), while causing micro-cracking by cleavage, are small enough as to not cause larger cracks, or dislodge grains by grain pullout.

6.4 Chemo-mechanical polishing (CMP)

The mechanism of material removal in the final stages of polishing by softer cerium oxide (CeO_2) is due to CMP. Thermal analysis of flash temperature and flash duration, as well as thermodynamic studies of the polishing process [Jiang, 1998], strongly suggest the possibility of CMP of Si_3N_4 by CeO_2 . The mechanism of material removal during the final stages of polishing by CeO_2 is due to CMP. Various abrasives were investigated for CMP of Si_3N_4 balls and

CeO₂ was found to be the most effective polishing medium. They investigated the underlying reasons for the superior finish obtained with CeO₂ abrasives. The most important function of CeO₂ is that it performs CMP of Si₃N₄ by participating directly in the chemical reaction (oxidization-reduction reaction) with Si₃N₄ work material leading to the formation of a thin SiO₂ layer. The heat for the chemical reaction is generated from the friction between the polishing shaft and the balls when rotating at high speeds. The hardness of CeO₂ is closer to that of the thin SiO₂ layer formed on the balls, but significantly lower than the silicon nitride work material (~1/3). It can thus remove the brittle SiO₂ reaction product effectively without damaging the substrate as no abrasion can take place by CeO₂ on silicon nitride. The kinetic action involves the removal of reaction products from the interface by subsequent mechanical action of flowing water and CeO₂. The chemical reaction could proceed on a continuing basis so long as the passivating layers are removed by mechanical action at the same time. The Si₃N₄ surface after CMP by cerium oxide may consist of an outer SiO₂ layer and an intermediary layer of silicon oxinitride (Si_xO_yN_z) on top of the silicon nitride substrate. Thus, tribo-chemical action instead of mechanical fracture is credited here for the extremely smooth and damage free surfaces accomplished on the Si₃N₄ balls.

6.5 Precision manufacturing process

Precision manufacturing process for finishing silicon nitride (Si_3N_4) bearing balls (with good sphericity and excellent surface finish to required size) to ANSI/ABMA 10, 7, 5, and 3 by MFP technology is presented in the following.

6.5.1 Out-of-roundness

It is found that accuracy of both apparatus construction and polishing set-up are critical for obtaining good sphericity of advanced ceramic balls in the MFP process. But these would not have much effect on the surface finish obtainable. In the MFP process, when larger diameter portions of ball enter the contact area, the load will increase and a larger amount of material from that point. This process continues till all the peaks disappear, resulting in improved sphericity.

The accuracy of the apparatus construction involves geometrical accuracy as well as relative positional accuracy of the setting used. The geometric accuracy depends on the accuracy of machine tools used. The relative positional accuracy depends on the adjustment and set-up of machine tools used in machining process. Regarding polishing and set-up accuracy, maintaining coaxiality between rotating axis of the polishing shaft and the polishing guide ring of the MFP apparatus is one of the most important criteria. In the following, these details are discussed briefly.

1. The geometrical accuracy of the main parts of the apparatus
 - a. Out-of-roundness of the internal cylindrical surface of the chamber.
 - b. Out-of-roundness of the cylindrical surface of the polishing shaft.

This depends upon the spindle rotational accuracy of the turning machine used for fabricating the chamber and the shaft, especially the inaccuracies in the spindle bearing, stiffness and thermal deformations.

The abrasive wear of the polishing shaft, the polishing float, and the urethane rubber ring during the polishing lead to improper polishing motion of the ball and can result in sphericity degradation. They should be re-machined or replaced periodically.

2. Relative positional accuracy of the apparatus
 - a. End surface of the shaft, which is the reference surface of the shaft to the drive spindle should be perpendicular to the rotating axis to minimize the additional inaccuracies in the rotational motion.
 - b. The tapered polishing surface of the shaft should be coaxial with the rotating axis. To satisfy the above mentioned requirements, ie, (a) and (b), during final precision machining stages, the machining of shaft cylindrical and conical polishing surfaces should be accomplished using one chuck mounting, taking the end surface as axial machining

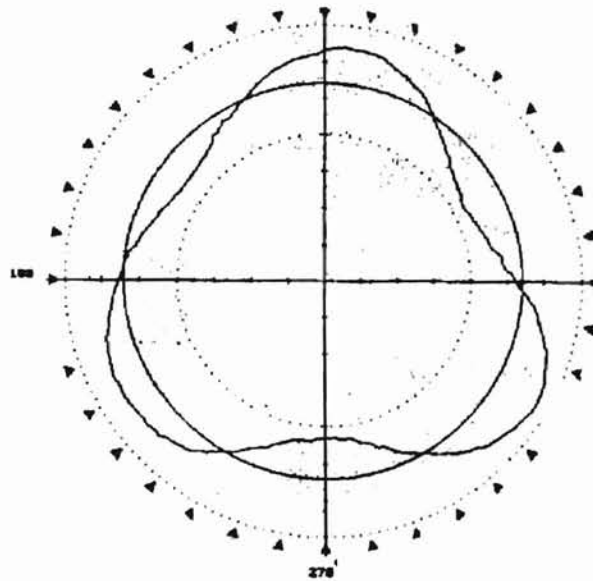
reference. To re-machine the conical polishing surface after wear, the shaft axis should be set up to be coaxial to the lathe axis by taking the cylindrical surface of the shaft, as the reference.

- c. The axis of the chamber wall should be perpendicular to the chamber base. Polishing chamber is used not only for containing the polishing fluid, but also for guiding the ball track as a guide ring. To preserve relation integrity, the machining of chamber should be done within one chuck mounting (without removing the work-piece from the lathe chuck) to machine ID and OD of the chamber for their concentricity and machine the end surface, to make perpendicularity of the end surface with respect to the chamber walls, which is the reference surface to ensure the chamber walls are perpendicular to the chamber base.

3. Coaxiality of the polishing shaft with chamber and the drive spindle

- a. Coaxiality between drive spindle and polishing shaft: Due to the abrasive wear in MFP process, periodically, the shaft has to be removed and polishing surface has to be re-machined. When the shaft is re-mounted to the drive spindle, great care must be used to align the shaft axis with the drive axis. It is preferred to re-grind the shaft, without removing the shaft from the spindle by setting up a grinding unit.

- b. Coaxiality between polishing shaft and polishing chamber: The mounting eccentricity between polishing shaft and polishing guide ring should be avoided. The improper setup or inadequate setup accuracy with even very small eccentricity is the main reason for the low sphericity. The given figure shows a typical triangle shape of a Si_3N_4 ball due to eccentricity between the polishing drive shaft and the guide ring.



The purpose of the above mentioned requirements is to keep the coaxiality between rotating axis of polishing shaft and polishing guide ring. This is the most frequent problem to cause bad sphericity results.

6.5.2 Surface finish

The methodology of fine mechanical polishing followed by chemo-mechanical polishing (CMP) is rather critical for obtaining excellent surface finish of advanced ceramic balls in the MFP process resulting in higher strength work material and reliability of the parts in service.

Chapter 7

Vibration monitoring and control

7.1 Introduction

As indicated in the previous chapters achieving good sphericity in the polishing of ceramic balls is dictated by various factors including coaxiality of the polishing shaft with the chamber and the drive shaft, the set up of the chamber for polishing, the accuracy with which the shaft and the chamber had been manufactured and the groove on the polishing shaft. The term “polish” and “polishing” in this chapter refers to one particular run during the whole process of finishing the balls from the as-received condition, unless stated otherwise. The settings are always subjected to human error, irrespective of the accuracy and care taken to perform the experiment. Even a slight parallax error can cause the setting to be eccentric to the axis of the drive shaft or the polishing shaft (both being already aligned). For good polishing, the groove on the spindle should have the same axis as that of the polishing shaft. A slight eccentricity in the setting of the chamber, with respect to the polishing shaft, can cause the balls to contact the tapered surface, higher on one side and lower on the other. This causes the axis of the groove to be inclined to the axis of the polishing shaft, subjecting the balls to alternate high and low loads, during rotation at high

speed. This is bound to worsen the sphericity of the balls, when compared to the sphericity before the polish.

Apart from manually setting the chamber there is no way one can check whether the chamber is satisfactorily coaxial with the polishing chamber. Till date, the only way to know if a polish has been good or not, is to measure the sphericity of the balls after the polish is done. In most cases this is not a desirable situation, particularly during the final stages of polish. If it is intended to improve the sphericity of the balls, with not much material to lose, an improper set up may worsen the sphericity as well as remove material. In such cases, the balls with an inferior sphericity and less material, compared to previous polishing run, are either polished again if material is available, or is discarded as it cannot be used with the current sphericity. This results in enormous wastage of material, labor, and precious polishing time. Some way to indicate the validity of a set up, before the polish is over, will at least help by saving precious material in case the set up is not good enough. The material saved, however minute, will be very valuable to allow further polishing, in order to improve the sphericity.

7.2 Validating setup using vibration

Every component or material involved in polishing has its own vibrating frequency, termed as natural frequency. Polishing is done by rotating the shaft at about 2000 – 3000 rpm, which in turn passes on its movement to the balls and the

fluid. At such high speeds, each component involved in polishing will be subjected to vibration. The resulting vibration may have more than one frequency at different amplitudes. Even if the vibration has a single frequency, it need not be the natural frequency of any component involved in the polish. The motion of the balls, the condition of the polishing shaft, the width of the groove on the shaft, the condition of groove on the float, flow of magnetic fluid and the rotational speed of the polishing shaft are some of the factors that affect the vibrating frequency of the polishing apparatus. A slight eccentricity in the shaft may cause the balls to rotate in a wavy fashion forcing the float to oscillate about its center. This induces vibrations with no single frequency, but multiple frequencies due to the ball, float, and the liquid motion. If the setup is correct, the balls rotate on a same plane (without any waviness) and so does the float. Hence such a rotation at high speed causes all the elements to vibrate in harmony, with a single frequency. This frequency, termed as the excitation frequency, need not be the natural frequency of any of the elements involved in the vibration.

The analysis is done, by recording the frequency spectrum (Frequency Vs Amplitude Vs Time) during the polish. This graph gives a cascading frequency Vs amplitude curve with respect to time. It is an aim of this work, to ensure the validity of set up during a run, by observing its frequency spectrum. With the help of this frequency spectrum, if it is diagnosed that the set up is not satisfactory, the polish can be stopped to prevent any wastage of material, which can be effectively used for improving the sphericity during the next polish. Since

the vibration monitoring sensors are placed on the apparatus as a whole, it is not possible to zero in on vibrations. It is also not possible to label the cause of the vibrations, since any one of the causes mentioned above can induce vibrations on the apparatus. Since the extremely bad sphericity of the balls can also cause such vibrations, even when all other conditions are satisfactory, the results are reliable only from a stage where the sphericity of the balls are such that they are not big enough to induce vibrations of high amplitude.

7.3 Set up for online vibration monitoring

The vibrations, from the polishing apparatus, were monitored using Vibroport 41 device from Schenck. Two screw-mountable accelerometer pick-ups, AS-020, were used. Two directions, one parallel to the axis of the polishing shaft, and the other perpendicular to it, were chosen to mount the accelerometer pick-ups. The two surfaces were machined to make sure that one of the surfaces is perpendicular to the wall of the chamber, and to ensure perpendicularity between them. Two holes were drilled and tapped, to accommodate the two screw heads. One of the accelerometer pick-ups was marked in order to mount it in the same position always. The leads from each pick-up were sent to separate channels on the Vibroport 41 equipment, and the two channels provide frequency spectrum without any dependence on one another. The schematic of the set up used in the experiment is shown in the figure 7.1. The equipment

allows the user to set the parameters for each channel either automatically or manually. Manual setting was chosen to ensure identical settings on both the channels to facilitate frequency spectrum comparison between the two channels.

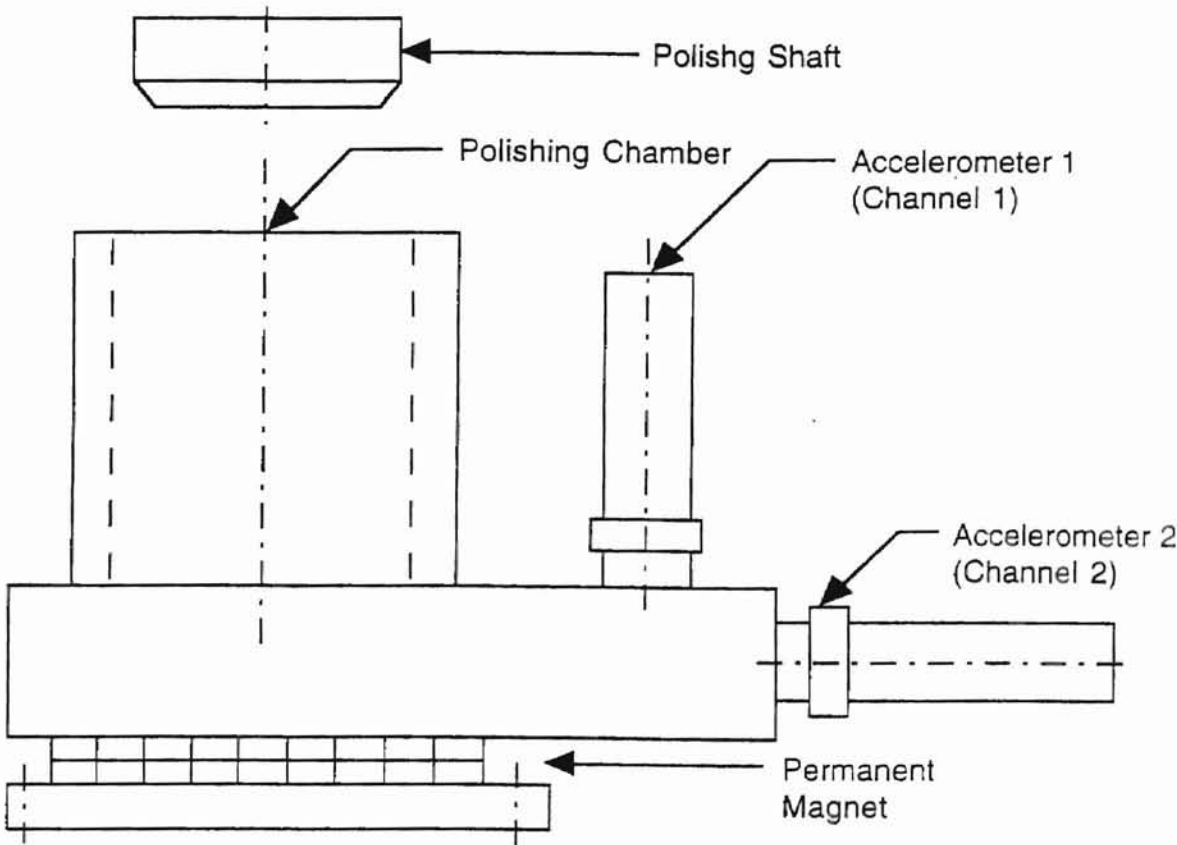


Figure 7.1: Set-up for online vibration monitoring and control

7.4 Parameters

Input:	Active
Type of Pick-up:	Acceleration
Sensitivity:	100 mV/g
Amplitude Unit:	m ² /s; rms
Amplitude Range:	Auto
Frequency Range:	0 – 2 kHz
Number of lines:	400
Window:	Flat top

The manual settings of each channel were done as follows. These settings are same for both the channels used in the study. The first parameter is to choose whether the pick-up is active or inactive. This has to be set inactive for the channel not in use, in case the user opts to use only one out of the two available channels. In our case this is set to active or both the channels. The type of pick-up comes next, which has choices like acceleration, velocity, displacement etc. Acceleration type pick up is chosen. The sensitivity of the accelerometer pick up is 100 mV/g as given by its specification. The amplitude is m²/s for acceleration and the type of calculation is root mean square (rms). Root mean square is the square root of the arithmetical average of a set of squared instantaneous values. The amplitude range is set to auto, to facilitate auto scaling of the frequency

spectrum with respect to the highest recorded amplitude. Moreover if an amplitude value is set, any amplitude more than the given value will be omitted, which is not desirable. The frequency range is selected as 0 – 2 kHz instead of auto, to make comparison of frequency spectrums easier. This range was selected based on previous experiments, as frequencies do not go beyond 2 kHz for normal polishing conditions. The number of lines on the spectrum along with the maximum and minimum frequencies determines the resolution on the spectrum. The resolution is given by $(F_{\max} - F_{\min}) / \text{number of lines}$. In our case the number of lines is set to 400, as 5 Hz / lines was taken to be adequate resolution for the purpose of this study. This means that there are 400 lines on the spectrum, each at 5 Hz from the other. The type of window was chosen as flat top filter, because this DSA window function provides the best amplitude accuracy for measuring discrete frequency components, which might be the case during polishing.

This frequency spectrum calculates the frequency and amplitude at various specified time intervals. The device allows selection of regular or irregular time intervals, during which the frequency Vs amplitude curve has to be generated for that time interval. All the polish runs were of 1-hour duration each. Hence for clarity of spectrum, 5 spectra over a time period of 180 seconds (3 minutes each), were recorded. Hence one full frequency spectrum with 5 spectra taken at an interval of 3 minutes will be generated every 15 minutes. The resulting frequency spectrum can be either saved or printed out with the help of an in-built printer. Due to memory constraints, the frequency spectrum of both

the channels will be printed out using special thermal paper, provided by Schenck, on the in-built printer. The printing operation takes approximately 4 minutes, during which no useful data is collected by the equipment. The process is like one 15-minute data collection, 4-minute printing out, followed by another 15-minute data collection and so on. Because of the time taken for print out, only 3 frequency spectrums are generated per polish, instead of 4.

Chapter 8

Results and discussion

The frequency spectrum Vs time graph obtained from the Vibroport 41 equipment has been used for analysis. Frequency (0 to 2 kHz) is taken on the x-axis, Amplitude is taken on the y-axis, and the time interval is taken on the z-axis.

Background vibrations of the environment in which the experiments were conducted, were taken before each run. A typical background vibration frequency spectrum has been given in figure 8.1. Polishing runs for finishing the balls were started and the frequency spectrum of the polishing runs behaved as expected, with many frequencies initially and one predominant frequency during the final 15-minute interval of the polish. During the setting of the 14th run, some discrepancies were introduced to study its effects. The chamber axis was set slightly eccentric to the axis of the polishing shaft, and high load of about 2 N/ball (normal load 1 N/ball) was applied for polishing. Figure 8.2 shows the frequency spectrum of the first 15-minute intervals on both the channels. The first 15-minute interval frequency spectrum shows a number of frequencies with high amplitudes on both the channels as expected. However the final spectrum (Figure 8.3) of that polish, shows more than

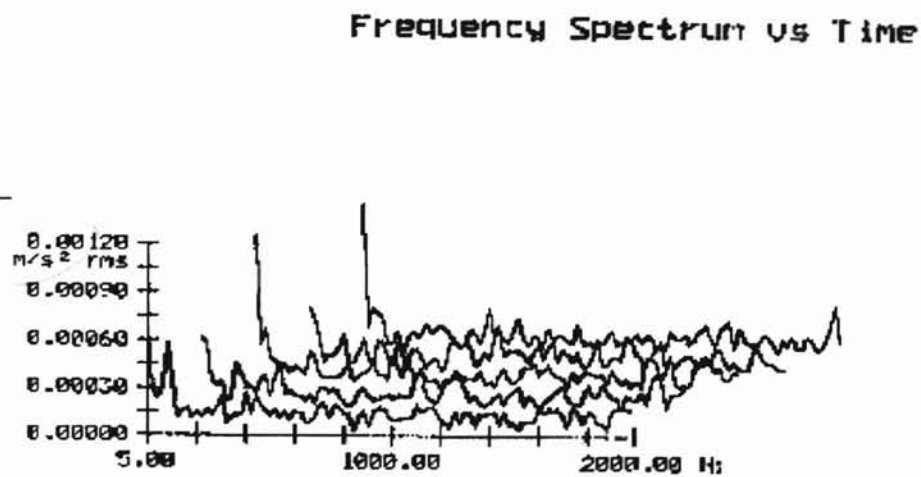
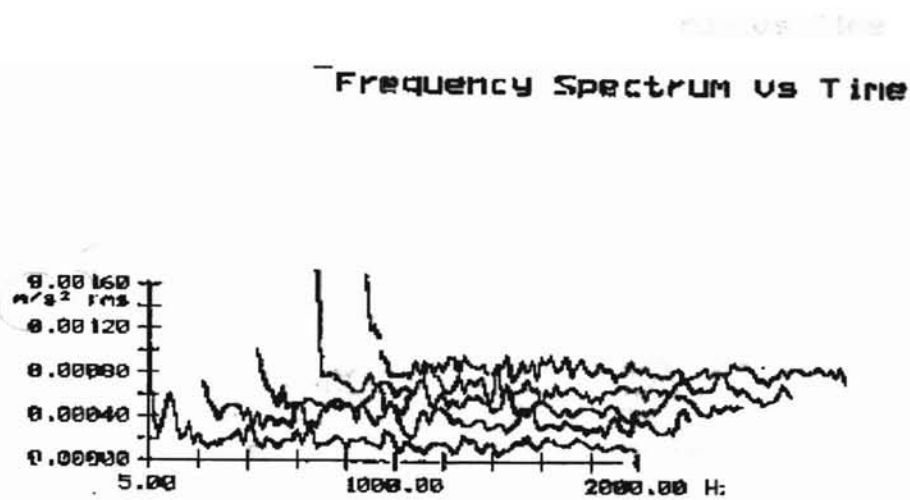
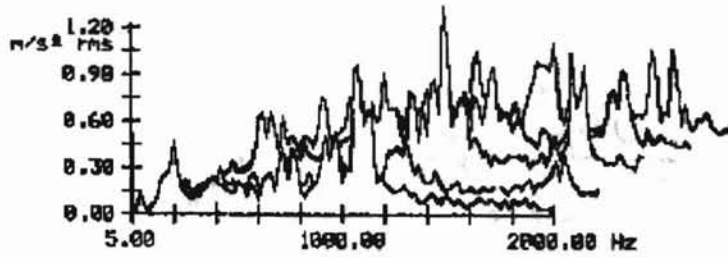


Figure 8.1: Typical background vibration of the environment in which polishing was performed

Frequency Spectrum vs Time



Frequency Spectrum vs Time

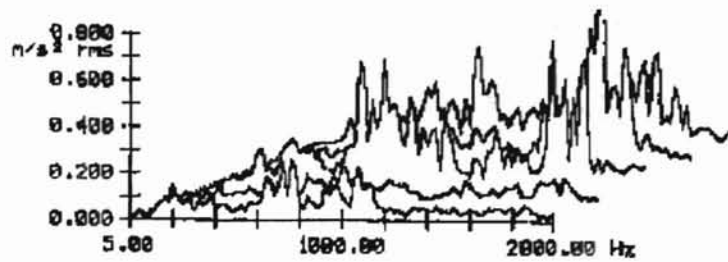
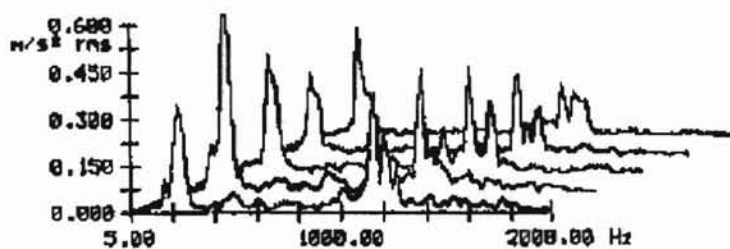


Figure 8.2: Frequency spectrum recorded during the first 15-minute interval during the 14th polishing run

Frequency Spectrum vs Time



Frequency Spectrum vs Time

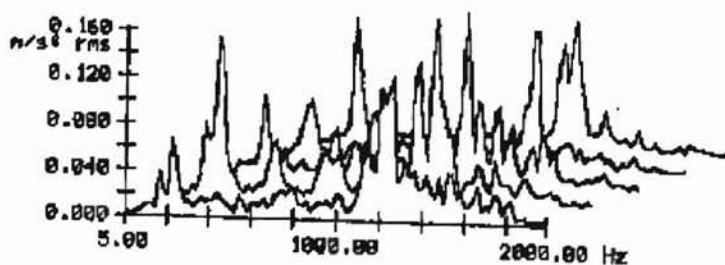


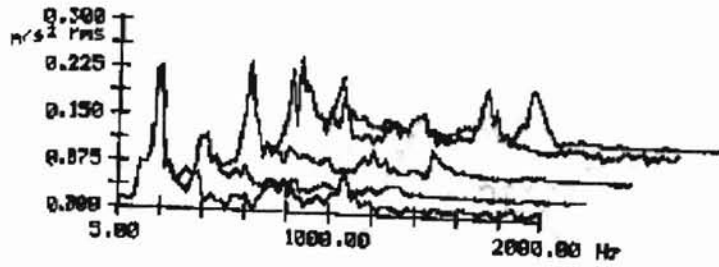
Figure 8.3: Frequency spectrum taken for the last 15-minute interval of the 14th polishing run

one predominant frequency. It shows two dominant frequencies with almost the same amplitude level in the first channel, whereas in the second channel it shows a number of frequencies at a lower amplitude level. As expected, the sphericity deteriorated from about $1.15\mu\text{m}$ to about $10\mu\text{m}$.

The 27th run showed a good decrease in the sphericity of the balls from about $0.9\ \mu\text{m}$ to $0.4\ \mu\text{m}$ and hence the frequency spectrum of this run was analyzed as follows. The frequency spectrum of this run is given in figures 8.4 and 8.5. The initial spectrum (first 15-minute interval) shows the presence of a number of frequencies. But the final spectrum shows the presence of one dominant frequency throughout the time interval of 15 minutes in the first channel. Even though some other frequencies are present, they can be neglected considering the amplitude with which they vibrate. In the second channel there are two dominant frequencies present, but their effect on the sphericity of the balls is negligible because of their low amplitude (less than $1/2$ of the amplitude of the first channel), proven by the fact that the sphericity has not deteriorated.

Out of all the runs of polishing done on the batch of 13 $17/32''$ balls, the 31st run seems to be the ideal behavior expected out of a good polishing set up and conditions. The frequency spectrum (shown in figures 8.6, 8.7 and 8.8) of the first 15-minute interval shows number of frequencies with inconsistent amplitudes throughout the time period of the frequency spectrum. Both the channels show the same behavior, with the amplitude of vibration in the second

Frequency Spectrum vs Time



Frequency Spectrum vs Time

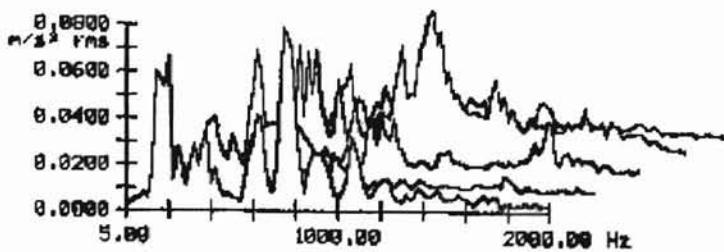
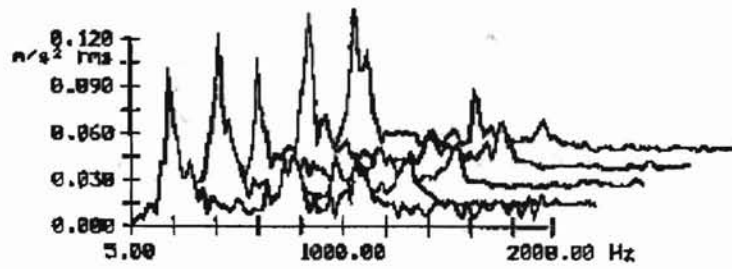


Figure 8.4: Frequency spectrum taken during the first 15-minute interval of the 27th polishing run

Frequency Spectrum vs Time



Frequency Spectrum vs Time

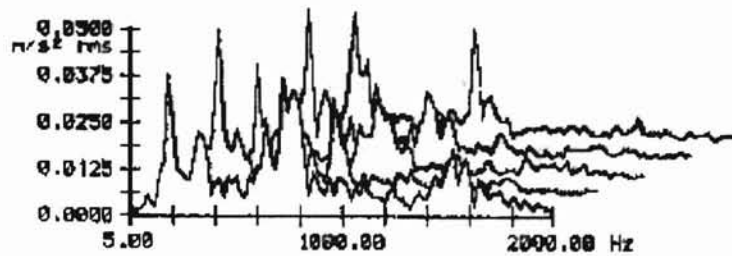
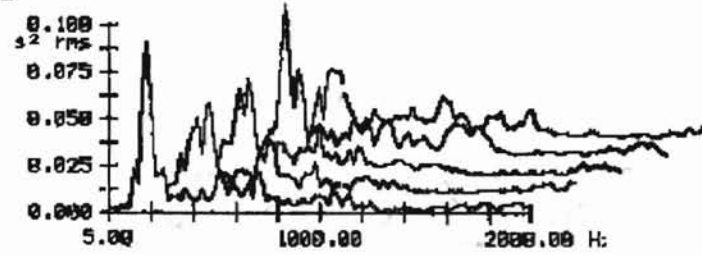


Figure 8.5: Frequency spectrum taken during the last 15-minute interval of
The 27th polishing run

Frequency Spectrum Us Time

05-10-1999



Frequency Spectrum Us Time

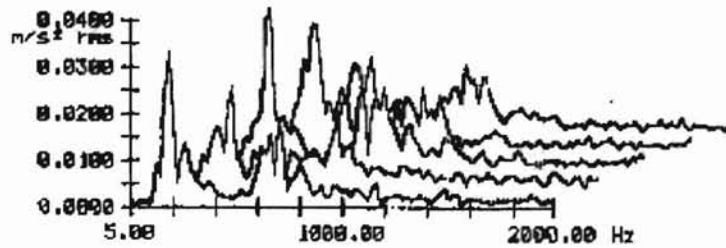
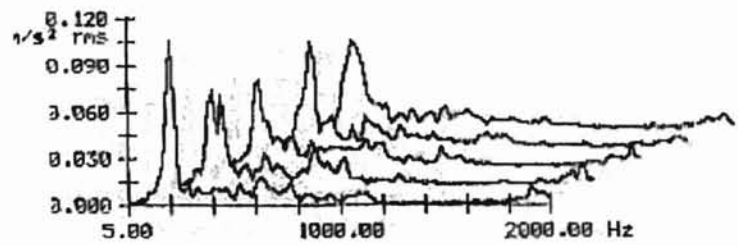


Figure 8.6: Frequency spectrum for the first 15-minute interval of the 31st polish

Frequency Spectrum vs Time

0



Frequency Spectrum vs Time

1

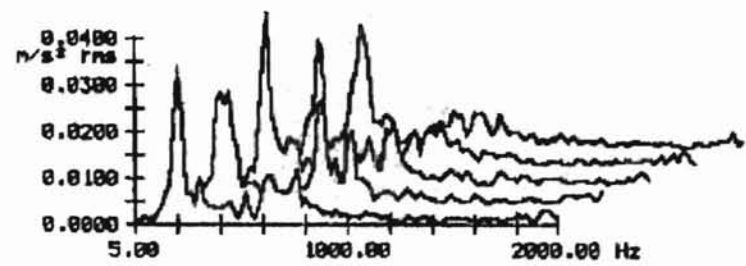
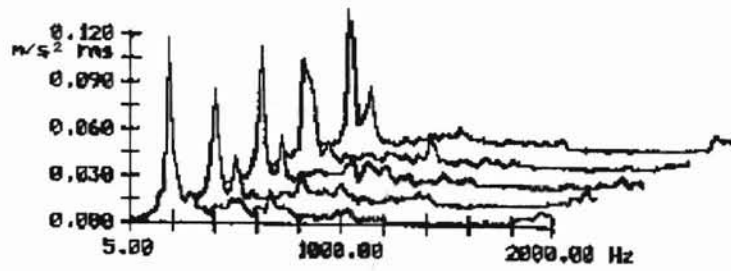


Figure 8.7: Frequency spectrum for the second 15-minute interval of the 31st polishing run

Frequency Spectrum vs Time



Frequency Spectrum vs Time

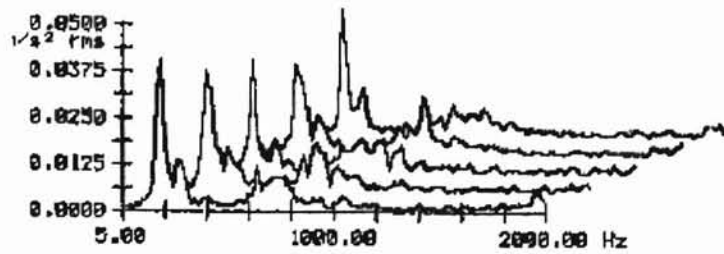


Figure 8.8: Frequency spectrum for the last 15-minute interval of the 31st polish

channel being lesser than the first one, which is always the case. The predominant frequency of this polish is seen as soon as the second interval, indicating that minimum error was introduced in setting the chamber with respect to the polishing shaft. The final 15-minute interval frequency spectrum further goes on to emphasize a single dominant frequency in both the channels, irrespective of their amplitude. In this case, the frequency spectrum of both the channels match exactly, with a single dominating frequency. In other runs, even if this was not the case, the sphericity results improved, thus indicating that the vibrations on the second channel of the equipment (accelerometer perpendicular to the shaft axis) played a lesser role in determining the sphericity of the balls. However it has been observed that if the frequency spectrum of the two channels match, great improvements in sphericity can be achieved. The best sphericity of the batch $0.25 \mu\text{m}$ was achieved in this run, and was maintained till the end. The sphericity results of the balls after the 14th, 27th and the 31st runs have been given in figures 8.9, 8.10, and 8.11 respectively.

In order to emphasize the importance of using such monitoring equipment, some tests were conducted on the 17/32" balls, after 4 polish runs, to remove the central band, with the designed shaft. A shaft designed for 9/32" balls was used to polish 17/32" balls. It was known that the ball would not contact the taper surface on the spindle, because its dimensions were designed for 9/32" balls. The vibration readings showed rather peculiar behavior. The results of this polish have been shown in figures 8.12 and 8.13. The frequency

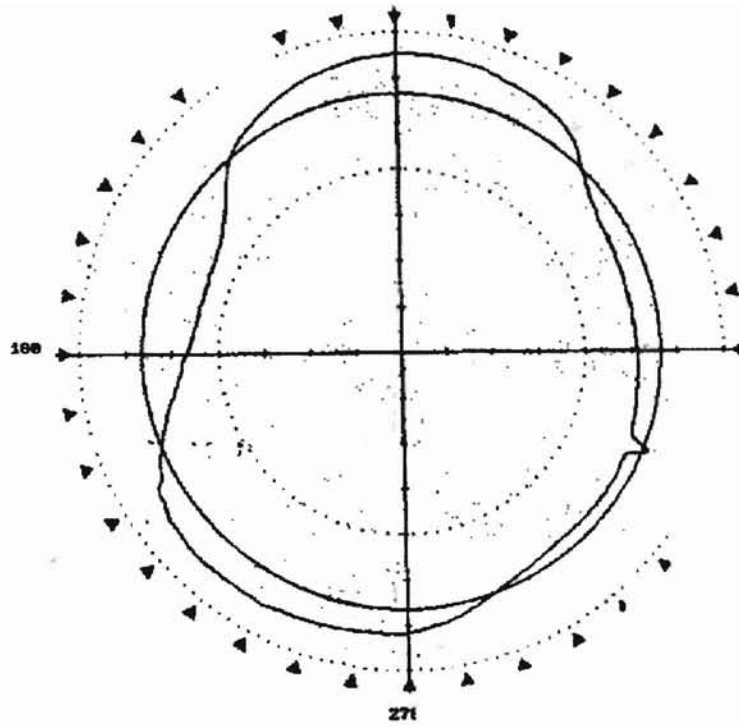


Figure 8.9: Sphericity of the balls after 14th polish. Sphericity value 10.3 μm

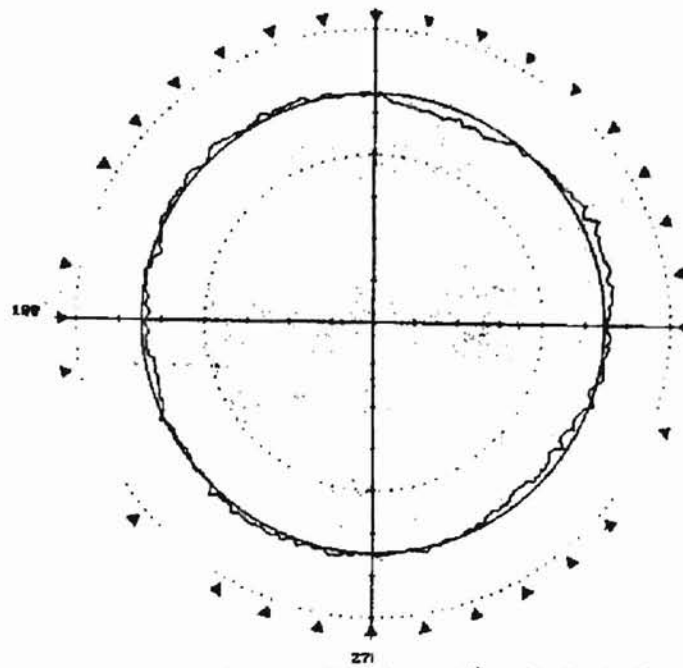


Figure 8.10: Sphericity of the balls after 27th polish. Sphericity value 0.35 μm

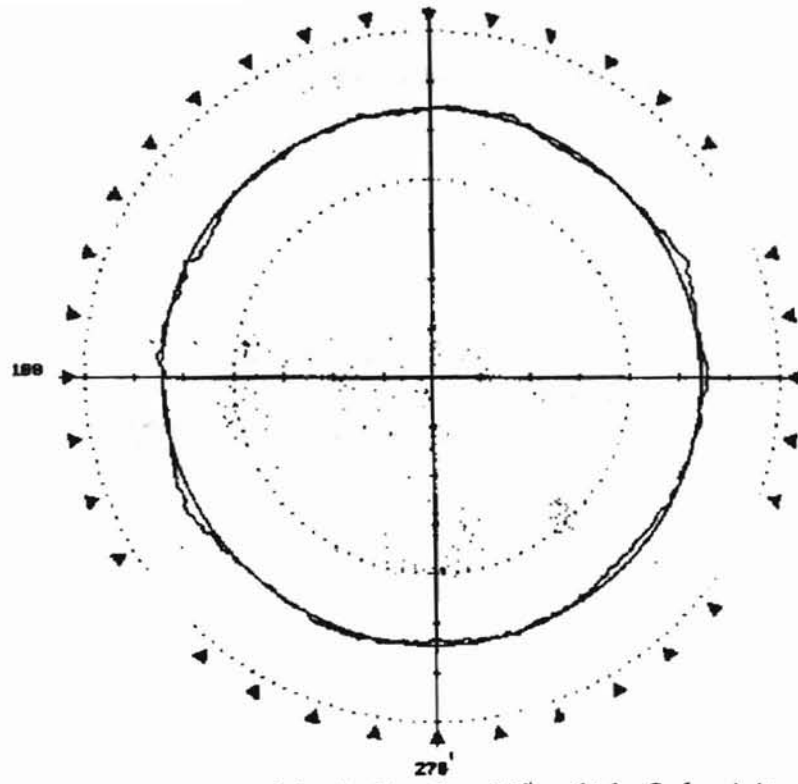
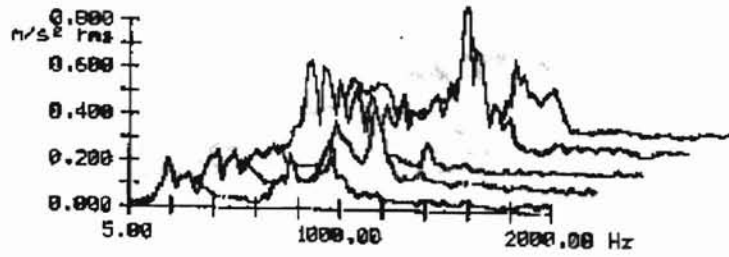


Figure8.11: Sphericity of the balls after 31st polish. Sphericity value 0.25 μm

Frequency Spectrum vs Time



Frequency Spectrum vs Time

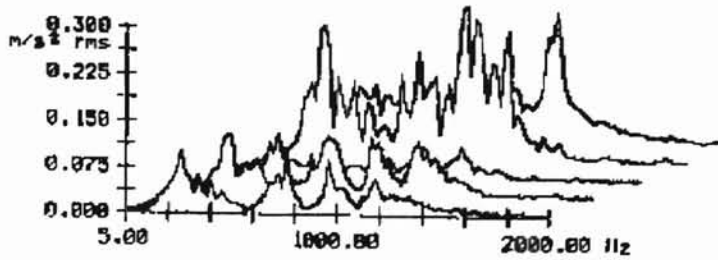
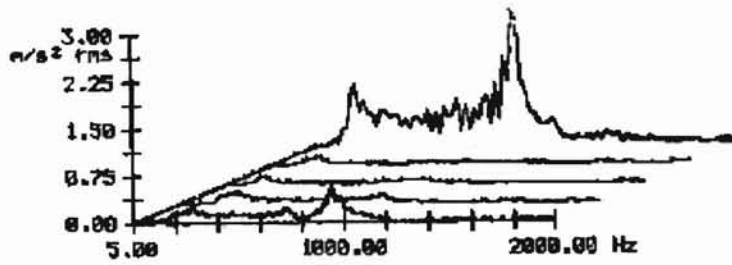


Figure 8.12: Frequency spectrum of the first 15-minutes of the polish test run done with an under sized spindle

Frequency Spectrum vs Time

-H



Frequency Spectrum vs Time

-H

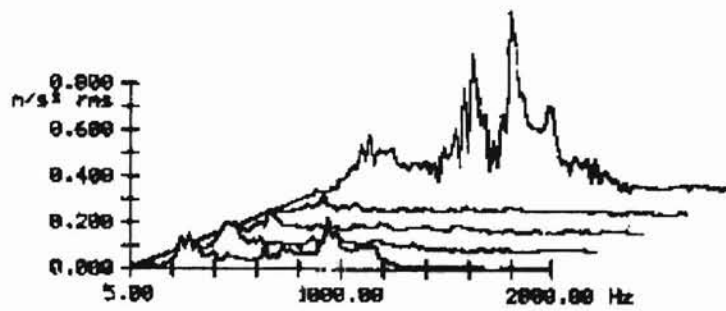


Figure 8.13: Frequency spectrum of the second 15-minute interval of the polish test run done with an under sized spindle

spectrum of this polish showed abnormal frequency bursts with very high amplitude. It does not have a single peak, but multiple frequencies with high amplitudes. A comparison of these graphs with frequency spectrum obtained from 31st run shows the abnormal nature of this frequency spectrum. Later analysis of the shaft showed that polishing had been taking place at the lower edge instead of the taper on the shaft. Hence the polish had taken place without proper force being applied on the balls, and they may not have been in three-point contact during the polish.

A general pattern of the frequency spectrum as the polish progresses has been observed. Initially, during the first 15-minute interval, the frequency spectrum shows the presence of a number of frequencies with various amplitude levels. This is because the set up, even if it is better than the previous one or not, is not repeatable. Hence initially, the balls have to either form a new groove, if the set up is bad, or settle down to the existing groove. Since this takes some time, the initial 15-minute frequency spectrum shows a number of frequencies with different amplitudes, which are usually high. The rms amplitude of a frequency spectrum is the highest for the first 15-minute interval, and goes on decreasing up to a particular level, for normal polish runs. This may be due to the fact that material removal is bound to be high initially due to inconsistent setups, and also because of the mechanism of material removal. Initially all the peaks in the ball surface get removed, and as the number of peaks reduces, the material removal becomes uniform all around the ball, and almost a constant.

As the process proceeds, the balls tend to settle down into a particular groove. If the axis of that groove coincides with the axis of the polishing shaft, the frequency spectrum shows a dominating peak at a particular frequency called the excitation frequency. This frequency is the one predominant frequency with which all the elements involved in the polishing vibrate. There may be other frequencies involved, but their magnitude would be negligible. This is the condition, with which best improvements in the sphericity of the balls have been observed. It has already been mentioned that the first 15-minute interval of the frequency spectrum will show number of frequencies with different magnitudes. For the polish to prove good, the final 15-minute interval (third) should show a dominant peak at the excitation frequency, with other frequencies of negligible amplitude. The intermediate frequency spectrum should be half way in between these two desirable conditions of the frequency spectrum. Of the two channels, channel 1, which has the frequency spectrum of the accelerometer parallel to the axis of the polishing shaft, showed more relevance to the sphericity of the balls. The readings from accelerometer perpendicular to the polishing shaft had very low amplitude when compared to the channel 1, with one or two frequencies. Hence observations and discussions will be concentrated on the first channel (accelerometer parallel to the axis of the polishing shaft), more than the second one. Since there is no exact formula or number to denote the characteristic of the frequency spectrum, the success in correct identification of an improper set up

from the spectrum is left to the perception of the researcher conducting the experiments.

These frequency spectrum graphs can indicate that a set up is improper, only if there is a considerable deterioration in sphericity. For example, monitoring vibrations can help in detecting set ups that can worsen the sphericity from 0.3 to 0.8 μm , but the frequency spectrum of set ups that can cause the sphericity to go from 0.3 to 0.35 μm , may not show any appreciable difference. Hence this monitoring system is particularly useful during the final stages of finishing a batch of balls. Since the tests were conducted only for about 1 hour, the fault detection in set up cannot be done before the second or even the final (third) 15-minute interval. But generally polish runs can go up to 1.30 hrs to 1.45 hrs, where such monitoring systems may prove to prevent or at-least reduce the wastage of ceramic ball material.

It can be observed that the online monitoring of vibrations to ensure the correctness of the set up can result in huge savings in terms of material available for polishing ceramic balls. Especially during the final stages of finishing of balls, it is important to have some material left to correct any out-of-roundness that may occur due to a bad set up. If the material available is not adequate to reduce the sphericity of the balls to the desired value within the specified diameter, it may require in either convincing the customer to accept balls with inferior sphericity, or scrapping the balls of that batch altogether, the latter being the case always. But the correct usage of this method depends on the experience of the

researcher. Being too careful may result in stopping the machine due to some aberration in the frequency spectrum, which may or may not have been due to faulty set up. This however does not affect the sphericity of the balls.

Over dependence on this system by a meticulous researcher can slow down the process of polishing a batch of balls due to frequent stoppage of runs. Hence the results of this system have to be used with some prudence and judgement on part of the researcher. With some experience the researcher may be able to tell whether it is affordable on his/her part to accept some deterioration in sphericity, taking into consideration the amount of material available in the balls, without stopping the run. If used properly, this technique is bound to improve the results, especially in a commercial system, where time is a main consideration. One need not waste time in removing material by deteriorating the sphericity of the balls. Instead after detection, another run with proper set up can be made, so that the time wasted in spoiling the sphericity of the balls and the time taken to bring it back into acceptable levels can be avoided.

8.1 Analysis made with respect to amplitude

Since Vibroport 41, without any additional software, does not have much capability to analyze the signal or graphs, all the following calculation was done manually. A slight possibility of scatter in the values is hence possible in such manual measurements. However it is worth mentioning that extreme care was

taken during the measurements of amplitude from the graphs. Since frequency spectrum from the first channel, whose pick-up is placed parallel to the axis of the shaft, has been found more representative of the polishing set-up and results, amplitude has been calculated only for the first channel. Moreover it has been discussed in the literature review that the amplitude of vibration parallel to the axis of the bearing is more when compared to the vibration in a perpendicular direction. Hence an effort to correlate the sphericity of the balls to the amplitude of vibration in that frequency spectrum has been discussed in the following. The manual method employed to calculate the amplitudes has also been explained.

8.2 Manual method of calculating the amplitudes

The length of the x-axis (frequency) is first measured with a centimeter scale. The x-axis of the last frequency Vs amplitude graph is drawn with the tip of the graph as the right-most point on the x-axis as one reference, and the bottom-most point of the curve as another. From the right-most point, the calculated length is marked off, in a line parallel to the original x-axis, to find the intersection of the x and y axes of that curve. The line denoting the intersection of the two axes is drawn first with the intersection points of the first and last graph as references. With this line as reference, the x-axes of all other graphs are drawn parallel to both the available x-axes. The peak of a curve is considered to be the actual rms amplitude for that curve. Hence the vertical distance between the x-

axis of a particular curve and its peak is measured with a scale. The calculated height is then translated onto the printed y-axis, and the amplitude value is read off as accurately as possible.

All significant peaks of a particular curve are taken into account in calculating the RMS value. The RMS value of a particular curve is the average of the RMS values of all the peaks in that curve. The RMS value of a specific frequency spectrum has been calculated as the average of the RMS values of all the curves. Hence a two-peaked curve has RMS value given as

$$\text{RMS of curve} = (\text{RMS of peak 1} + \text{RMS of peak 2}) / 2.$$

RMS value of a frequency spectrum is given as

$$\text{RMS of freq. Spec.} = \text{RMS of (curve 1 + curve 2 + curve 3 + curve 4 + curve 5)} / 5.$$

8.3 Analysis of Amplitude Vs Sphericity curve

The frequency spectrum of runs apart from 14, 27, and 31, are selected at random to be used for data of this graph. Due to error in data collection for runs 17 through 24, these data were unavailable for drawing the graph shown in figure 8.14. The data shows a linear trend in the graph between amplitude of vibration and sphericity of balls. The sphericity results correspond to the values after that particular run, which gave out the shown amplitude of vibration during the run. The lowest amplitude of vibration is seen when the best sphericity of balls is obtained, i.e. when there are least number of lobes present in

the surface profile of the balls. However it can be observed, that the validity of a polish can be verified only with reference to the previous run. If the sphericity of a ball is bad, and the set-up is good, the amplitude of vibration may be still high due to the presence of lobes on the surface due to out-of-roundness. Hence if consecutive polishing runs are done with minimum error, the amplitude of vibration will go on decreasing.

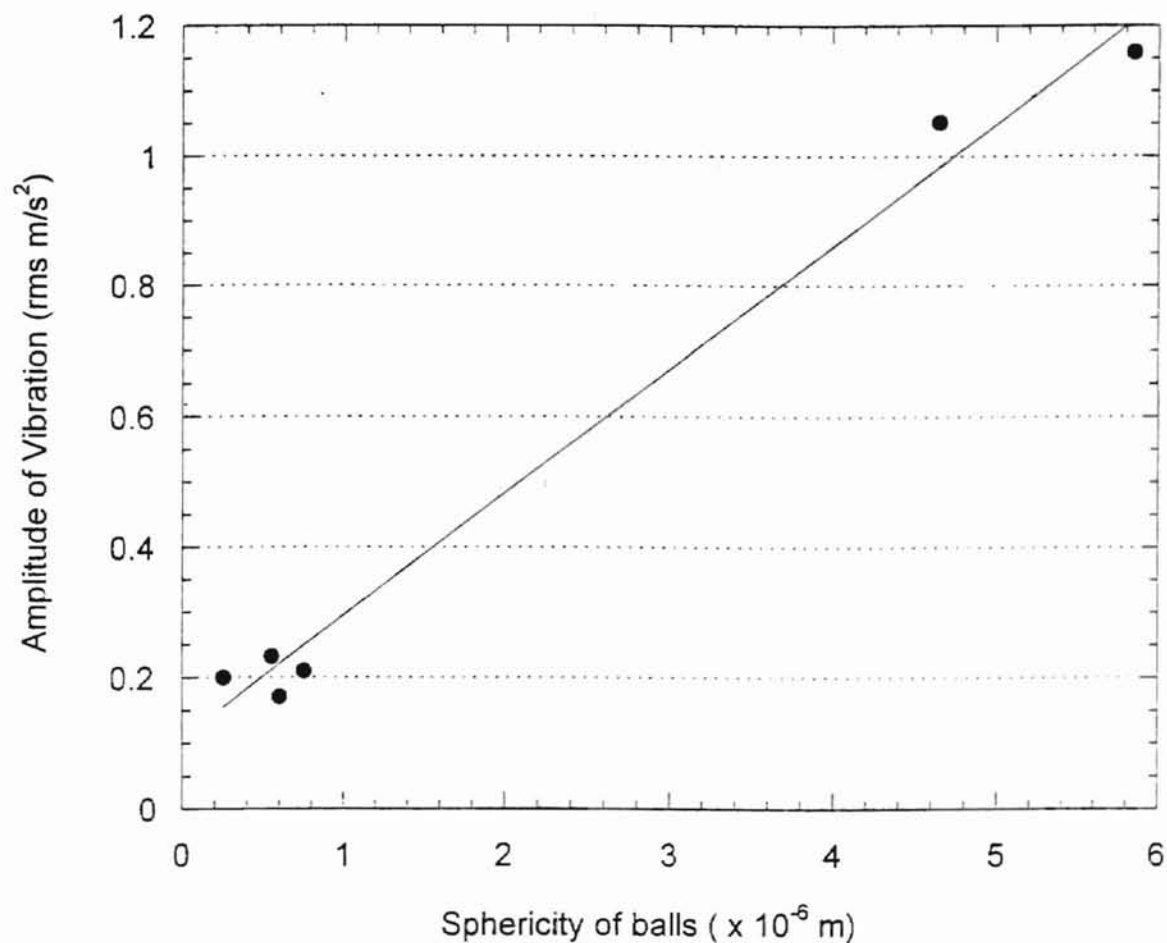


Figure 8.14: Graph of Sphericity of balls Vs Amplitude of vibration.

If the amplitude of vibration of a particular frequency spectrum is less than the corresponding frequency spectrum of the previous run, it means that the set-up for the current run is effective in removing or reducing the out-of-roundness of the ball, when compared to the previous value of sphericity. Any discrepancy in the linear decreasing trend indicates that the set-up of the polishing is ineffective in reducing the sphericity of the balls. A non-decreasing trend in the amplitude of vibration of consecutive polishing runs may not mean that the set-up is the only aspect faulty in the whole apparatus. It just means that the polish is not going on properly, and is not effective in reducing the sphericity of the balls. But however the set-up is the major cause of bad sphericity from a polishing run.

The intermediate data in the range $1 - 4 \mu\text{m}$ sphericity, an important region, were not available due to error in retrieving data in that range. The data in that range determines the trend whether it can be linear or exponential. Since the sphericity of the balls decreases during polishing, due to micro-fracture of the ceramic material, and also because the peaks and lobes on the surface of the ball act as vibration generators, it seems to be logical to predict the trend as linear rather than exponential.

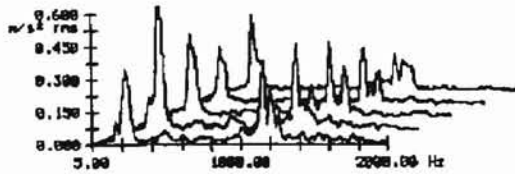
The frequency of the dominant peak observed at about 200 Hz may be caused due to the rotation of the balls. Since the polishing is done at a speed of 3000 rpm, the frequency of rotation is 50 Hz. The final diameter of the balls is

! approximately $\frac{1}{2}$ " and the diameter of rotation of the balls within the polishing chamber is approximately 2". Hence the diameter of rotation of the balls is approximately 4 times the diameter of the balls. Multiplying the frequency of rotation (50 Hz) with the ratio of ball diameter to diameter of rotation (4), we get the frequency as 200 Hz. This may be the reason for the dominant peak at approximately 200 Hz. It would be interesting to study if the frequency of the dominant peak changes with the sphericity of the balls. The frequency spectrum graphs have been shown in figure 8.15, alongside with the sphericity of balls that caused vibrations.

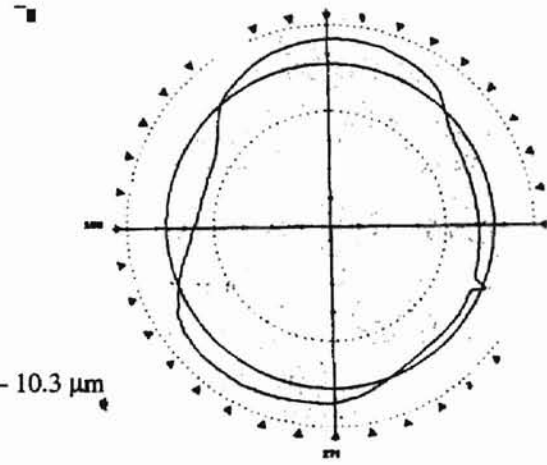
Frequency spectrum Vs time graph for last 15-minute interval of channel 1 – 14, 27, and 31st runs

Sphericity of the ball after that particular polish

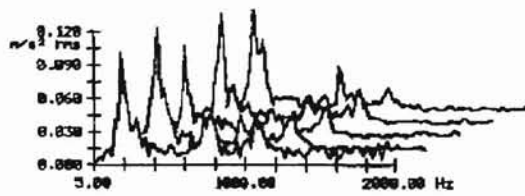
Frequency Spectrum vs Time



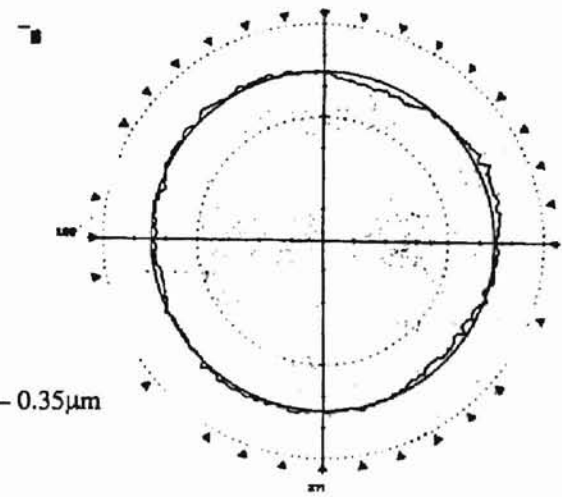
14th run - Calculated rms amplitude 1.05 m²/s, Sphericity – 10.3 μm



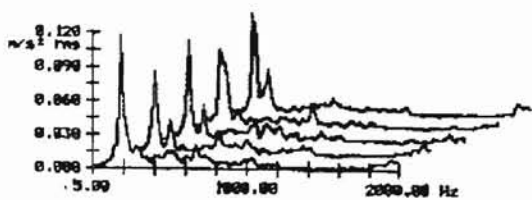
Frequency Spectrum vs Time



27th run – Calculated rms amplitude 0.232 m²/s, Sphericity – 0.35 μm



Frequency Spectrum vs Time



31st run – Calculated rms amplitude 0.2 m²/s, Sphericity – 0.25 μm

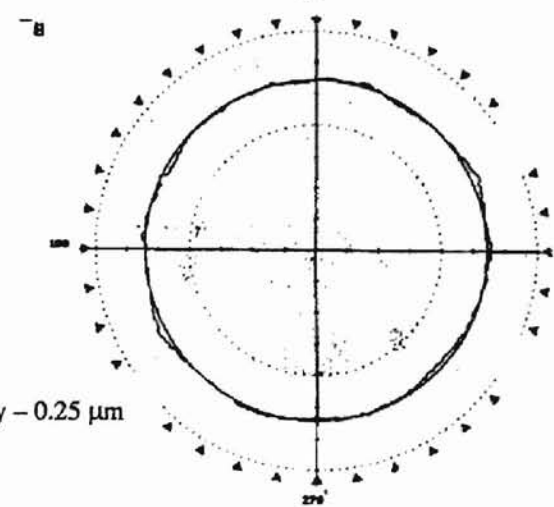


Figure 8.15: Comparison of Frequency spectrum Vs Time graph with Sphericity

Chapter 9

Conclusions

1. Magnetic float polishing (MFP) of Si_3N_4 balls for bearing applications using fine mechanical polishing followed by chemo-mechanical polishing (CMP) is an efficient and cost effective manufacturing technology for producing high quality, because of using high polishing speed, small and controlled polishing force, flexible support and chemo-mechanical action.
2. The apparatus used in the investigation can be used for polishing ceramic balls effectively, with few modifications in the dimensions of the polishing shaft, without any change in the process previously used for balls of different sizes.
3. A new polishing shaft was successfully designed for polishing 17/32" ceramic balls, with the dimensions of the existing chamber being the main constraint. The inner and outer diameters of the polishing shaft are determined by the diameter of the balls to be polished. The gap between the chamber and the outer diameter of the shaft has to be less than or equal to half the diameter of the balls polished. The gap between the inner diameter of the shaft and the diameter of the chamber has to be greater than or equal to the sum of the diameter of the balls and the thickness of the rubber sheet.

4. Magnetic float polishing was successfully performed to produce 17/32" balls using the shaft designed. Mechanical polishing was done initially using coarse B₄C (500 grit) and SiC (800 grit) abrasives with emphasis on material removal. Semi finishing was done next using finer SiC abrasive (1000 and 1200 grit) to improve the sphericity of the balls without removing much material. Finishing was done using B₄C (1500 grit) with emphasis on sphericity of the balls. Chemo-mechanical polishing (CMP) was performed next to improve the surface quality of the balls with CeO₂ abrasive. A sphericity of 0.25 μm was successfully obtained.
5. A good set up is indicated by one dominant frequency, called the excitation frequency, in the whole frequency spectrum. Each spectra should have the same dominant frequency, may be in slightly differing amplitudes, within a spectrum. The presence of more than one dominant frequency indicate an improper set up, in other words, an eccentricity between the axes of the polishing chamber and the shaft.
6. During the initial 15-minute interval more than one frequency is seen in the frequency spectrum due to inconsistencies in set up due to human error and non-repeatability of polish settings. A number of frequencies in single spectra with different amplitudes may be present. This initial spectrum is not a representative of the set up, as the inconsistency cannot be avoided with the present technique used. After the ball settles down into a specific groove, and if the polishing set up is good, an excitation frequency will be seen in the

frequency spectrum. All other frequencies present will have negligible amplitude.

7. The Sphericity Vs amplitude of vibration graph shows a linear trend of values. It indicates that the amplitude of vibration decreases linearly with decrease in sphericity. This is due to the reduction in number of peaks or lobes, at lower sphericities, which act as vibration generators during the polish.

8. Any discrepancy in the given behavior indicates a faulty set-up and hence the machine can be stopped without deteriorating the sphericity of the ceramic balls any further. This technique can be very useful to prevent wastage of magnetic fluid, abrasives, ceramic ball material and time, by indicating improper set up by vibrations generated during polishing.

Chapter 10

Future Work

Magnetic float polishing can be a cost-effective process for finishing Si_3N_4 balls for bearing application. A batch of balls can be finished in about 16 to 20 hours compared to several weeks by conventional polishing. Also, diamond abrasive is not required for this process. Faster polishing times and the use of abrasives other than diamond would significantly reduce the overall costs of manufacture. Also, implementation of this technology would not be capital intensive as it can be used, by incorporating in existing equipment.

10.1 Setting up of polishing apparatus by using lasers

But the current technique used for setting up the polishing apparatus is a highly time consuming and has very low repeatability. The current process relies heavily on the skill of the researcher to set the chamber axis in alignment with that of the polishing shaft. Moreover fatigue comes in the way of setting up the chamber and human error becomes unavoidable. In commercial situations a foolproof technique to set up the chamber will be of great use, to improve the process and working time efficiently.

A laser aligning system is hereby proposed to accurately align the axis of the chamber to the axis of the polishing shaft. A laser beam receiver is placed on the spindle accurately aligned with its axis. Its corresponding beam emitter is fitted on the chamber, accurately on its axis. This aligning can be done manually or using servo-motors on the feed directions. However this requires that the chamber not be removed from its position so that the accuracy of the laser beam emitter and its receiver is not disturbed. In addition to this some alterations have to be made to the apparatus to assist cleaning of chamber and removal of balls for each polish.

With such a system, aligning the chamber with the polishing shaft is bound to take considerably less time when compared to the current technique of setting manually. Repeatability of settings increases the efficiency of the system and is not subjected to unavoidable human errors. Not much study has been conducted as such to strengthen this technique, however this is just a proposal by the author, which seems to be feasible.

10.2 Vibration monitoring and control using advanced software

The vibration monitoring apparatus used for this study is inadequate for the analysis and comparison of various frequency spectrums. Since this was just a primary study to find out the consistency of results picked-up during polishing, no software was used for this work. Now that the validity of the

results has been confirmed by this work, an effort to analyze the frequency spectrum in much more depth is required. An effort should be made to detect the type of fault, if other than set up, and prevent further degradation of the sphericity of the balls. Any fault other than set up should be looked into, and vibration spectrums should be used effectively to distinguish improper polish runs, due to faulty set up or due to any other factor. Vibration patterns should be identified for specific type of faults, by transposing one frequency spectrum over another one to analyze the results.

References

Baghavatula, S. R., and Komanduri, R., "On Chemo-mechanical Polishing of Silicon Nitride with Chromium Oxide Abrasive," *Philosophical Magazine A*, 74/4, 1996, 1003-1017.

Buchner, K., "A Comparison of Spindle Ball Bearings with Steel or Ceramic Balls for Very High Speed Applications," *Creative use of Bearing Steels*, ASTM STP 1195, J. J. Hoo, ED., American Society for Testing Materials, Philadelphia, 1993, 121-133.

Burrier, H. I. and Burk, C., "Fatigue and Wear Behavior of NBD-200 Silicon Nitride Balls," *Ceramic Bearing Development*, WL-TR-96-4015.

Childs T. H. C., Jones, D. A., Mahmood, S., Kato, K., Zhang, B., and Umehara, N., "Magnetic Fluid Grinding Mechanics," *Wear*, 175, 1994a, 189-198.

Childs T. H. C., Mahmood, S., and Yoon, H. J., "The Material Removal Mechanism in Magnetic Fluid Grinding of Ceramic Ball Bearings," *Proc. Of I. Mech. E. London*, 208, No.B1, 1994b, 47-59.

Childs T. H. C, Mahmood, S., and Yoon, H. J., "Magnetic Fluid Grinding of Ceramic Balls," *Tribology International*, 28, No.6, 1995, 341-348.

Hou, Zhen-Bing and Komanduri, R., "Magnetic Field Assisted Finishing of Ceramics – Part I: Thermal Model," *Trans ASME, J. of Tribology*, 120, Oct. 1998, 645-651.

Hou Zhen-Bing and Komanduri, R., "Magnetic Field Assisted Finishing of Ceramics – Part II: On the Thermal Aspects of Magnetic Float Polishing (MFP) of Ceramic Balls," *Trans ASME, J. of Tribology*, 120, Oct. 1998, 652-659.

Hou, Zhen-Bing and Komanduri, R., "Magnetic Field Assisted Finishing of Ceramics – Part III: On the Thermal Aspects of Magnetic Abrasive Finishing (MAF) of Ceramic Rollers," accepted for publication in *Trans ASME, J. of Tribology*, 120, Oct.1998, 660-667.

Inasaki, I., "Grinding of Hard and Brittle Materials," *Annals of the CIRP*, 36/2, 1987.

Jiang Ming and Komanduri, R., "Application of Taguchi Method to Determine Polishing Conditions in Magnetic Float Polishing," *WEAR*, 213, 1997, 59-71.

Jiang Ming and Komanduri, R., "Finishing of Si_3N_4 Balls for Bearing Applications," WEAR, 215, 1998, 267-278.

Jiang Ming and Komanduri, R., "On the Chemo-mechanical Polishing (CMP) of Silicon Nitride Bearing Balls with Water Based CeO_2 Slurry," Trans ASME, J of Engg Mat. and Tech., 120, Oct. 1998, 304-312.

Jiang Ming, Wood, N., and Komanduri, R., "On the Chemo-mechanical polishing (CMP) of Silicon Nitride (Si_3N_4) workmateiral with various abrasives," WEAR, 220, 1998, 59-71.

Jiang Ming, "Finishing of Advanced Ceramic Balls for Bearing Applications by Magnetic Float Polishing (MFP) Involving Fine Polishing Followed by Chemo-Mechanical Polishing (CMP)," Masters Thesis, July 1998.

Katz, R. N. and Hannoosh, J. G., "Ceramics for High Performance Rolling Element Bearings: A Review and Assessment," Int. J. of High Technology Ceramics, 1, 1985, 69-79.

Komanduri, R., "On the Mechanisms of Material Removal in Fine Grinding and Polishing of Advanced Ceramics," Annals of CIRP, 44/1, 1996.

Komanduri, R., Umehara, N., and Raghunandan, M., "On the Possibility of Chemo-mechanical Action in Magnetic Float Polishing of Silicon Nitride," *Trans ASME, J of Tribology*, 118, 1996, 721-727.

McColm, I. J., "Ceramic Science for Materials Technologists," 1983, 107-114.

Raghunandan, M., Noori Khajavi, A., Umehara, N., and Komanduri, R., "Magnetic Float Polishing of Advanced Ceramics," *Trans ASME, J of Manf. Sci. and Engg.*, 119, 1997, 520-528.

Richard L. Schultz, "Forcing frequency identification of rolling element bearings," *Sound and Vibration*, May 1990, 16-19.

Tallian, T., "The mechanics of rolling-element bearing vibrations," *ASME Paper No. 58-A-292*, November, 1958, New York.

Tallian, T. E. and Gustafsson, O. G., "Progress in rolling bearing vibration research and control," *ASLE Transactions*, 1965, 195-207.

Tani, Y. and Kawata, K., "Development of High-efficiency Fine Finishing Process Using Magnetic Fluid," *Annals of CIRP*, 33/1, 1984, 217-220.

Umehara, N., and Kato, K., "Principles of Magnetic Fluid Grinding of Ceramic Balls," *Applied Electromagnetics in Materials*, 1, 1990, 37-43.

Umehara, N., Kato, K., and Kanagawa, I., "Magnetic Fluid Grinding of Ceramic Flat Surfaces," *Electromagnetic Forces and Applications*, Elsevier Science Publishers, 1992, 143-146.

Umehara, N., "Magnetic Fluid Grinding – A New Technique for Finishing Advanced Ceramics," *Annals of CIRP*, 43/1, 1994, 185-188.

Umehara, N., and Komanduri, R., "Magnetic Fluid Grinding of HIP-Si₃N₄ Rollers," *WEAR*, 192, 1996, 85-93.

Vance John, M., "Rotordynamics of Turbomachinery, John Wiley & Sons Inc., New York, 1988.

Vora, H., and Stokes, R. J., "Study of Mechano-chemical Machining of Ceramics and the Effect on Thin Film Behavior," Rept. No. N00014-80-C-0437-2, 1983.

Wang, J. C. and Hsu, S. M., "Chemically Assisted Machining of Ceramics," *J. of Tribology*, 116, 1994, 423-429.

Yasunaga, N., Tarumi, N., Obara, A., and Imanaka, O., "Mechanism and Application of the Mechanochemical Polishing Using Softer Powder," Science of Ceramic Machining and Surface Finishing-II, Ed. Hockey, B. H., and Rice, R. W., NBS Special Publication, No. 562, 1979, 171.

Yhland, E. M., "Waviness Measurement – An instrument for quality control in rolling bearing industry," Proc Instn Mech Engrs, 182-3k, 1967-68, 438-445.

VITA

Srihari Raghava Rao

Candidate for the Degree of

Master of Science

**Thesis: FINISHING OF CERAMIC BALLS BY MAGNETIC FLOAT POLISHING
WITH ONLINE VIBRATION MONITORING AND CONTROL**

Major Field: Mechanical Engineering

Biographical:

Personal Data: Born in Madras, Tamilnadu, India, on September 13, 1976, the son of Raghava Rao and Premasudha.

Education: Received Bachelor of Engineering degree in Mechanical Engineering from University of Madras, Tamilnadu, India, in May 1997. Completed the requirements for the Master of Science degree with a major in Mechanical and Aerospace Engineering at Oklahoma State University, Stillwater, Oklahoma in December, 1999.

Experience: Graduate Research Assistant in mechanical and Aerospace Engineering Department, Oklahoma State University, Stillwater, Oklahoma, January 1998 – August 1999.